Assessing the redox state of the plastoquinone pool in algae and cyanobacteria via OJIP fluorescence: perspectives and limitations

Tomáš Zavřel[1], Anne-Christin Pohland[2], Tobias Pfenning[3,4], Anna Barbara Matuszyńska[3,4], Szilvia Z. Tóth[5], Gábor Bernát[6], Jan Červený[1]

[1]Department of Adaptive Biotechnologies, Global Change Research Institute, Czech Academy of Sciences, Brno, Czechia

[2]Bio-Inspired Energy Conversion, Technical University Darmstadt, Darmstadt, Germany

[3]Computational Life Science, Department of Biology, RWTH Aachen University, Aachen, Germany

[4]Cluster of Excellence on Plant Sciences, Heinrich Heine University Düsseldorf, Düsseldorf, Germany

[5]Laboratory for Molecular Photobioenergetics, Institute of Plant Biology, HUN-REN Biological Research Centre, Szeged, Hungary

[6]Aquatic Botany and Microbial Ecology Research Group, HUN-REN Balaton Limnological Research Institute, Tihany, Hungary

Corresponding author: Tomáš Zavřel

Abstract

Background: The redox state of the plastoquinone pool (PQ-redox) acts as a central element in a variety of intracellular signal pathways. Several methods for determining PQ-redox have been established. Although some methods are fully quantitative, such as those based on liquid chromatography, they are typically sensitive to sample preparation. Here, we critically evaluate the use of fast chlorophyll *a* fluorescence induction kinetics (the so-called OJIP transient) for semi-quantitative PQ-redox assessment in algae (*Chlorella vulgaris*) and cyanobacteria (*Synechocystis* sp. PCC 6803). The method, based on the evaluation of relative fluorescence yield at the J-step of the OJIP transient (V_J), has already been reported; however, thus far, it has been used mostly for studying dark-acclimated leaves, which limits its range of use.

Results: In this work, we show that the OJIP transient can be used for semi-quantitative estimation of PQ-redox in algal and cyanobacterial cell cultures, in addition to plants. We further show that it can reflect PQ-redox in both dark-acclimated and light-acclimated samples. To estimate PQ-redox in light-acclimated cells, we introduce a new parameter V_J'. This parameter is derived from F_O', F_J' and F_M' values - the fluorescence yields at the O and J steps of the OJIP transient, and the maximum fluorescence yield, respectively, measured in light-acclimated samples. Our systematic comparison of Multi-Color PAM, AquaPen, and FL 6000 fluorometers demonstrates that accurate measurement of V_J and V_J' in algal and cyanobacterial cultures requires low culture density and a high-intensity saturation pulse. We further show that with increasing light intensity to which the cells are exposed, the state of photosystem II (PSII) changes due to light-induced reduction of quinone A (Q_A^-) and conformational changes, which in turn influence both the sensitivity and dynamic range of the V_J' parameter towards PQ-redox assessment. A comparison of fluorescence curves in algae and cyanobacteria revealed high homeostatic control over PQ-redox in *Synechocystis* sp. PCC 6803, maintained by terminal oxidases present at the thylakoid membrane.

Conclusions: While certain limitations exist, our critical assessment suggests that the OJIP method has great potential to become a routine tool for semi-quantitative PQ-redox assessment under a wide range of experimental conditions.

Keywords:

OJIP curves, Chlorophyll *a* fluorescence, Redox state, PQ pool, Photosystem II, Quinone A, *Synechocystis*, *Chlorella*

Background

Photosynthesis is a fundamental process on Earth that provides energy (and produces biomass) for almost the entire food chain. During photosynthesis, light energy is captured by light-harvesting antennas. The captured energy is ultimately transferred to the reaction centers (special pair of chlorophyll molecules) of the photosystems where charge separation takes place (1). Using the positive charges created, water is split into molecular oxygen and protons at the oxygen evolving complex of photosystem II (PSII) (2), while the released electrons are passed through the photosynthetic electron transport chain (PETC) towards photosystem I (PSI) and to the terminal electron acceptors such as $NADP^+$. The mobile, membrane-bound PETCelectron carrier, plastoquinone (PQ), accepts electrons from PSII, and transfers them (in the form of plastoquinol, PQH_2) primarily to cytochrome b_6/f (Cyt b_6/f), from which they are further transferred to PSI through water soluble electron carriers, plastocyanin or cytochrome c_6 (3). The redox state of the PQ/PQH_2 pool (PQ-redox hereafter), i.e. the portion of PQ reduced, relative to the portion of PQ oxidized, has an important signaling function, triggering a variety of metabolic processes, including light acclimation, biosynthesis of metabolites, and gene expression (4).

The PQ/PQH_2 pool can be reduced and oxidized by several light-dependent and light-independent electron transport processes. Besides linear electron flow, these include cyclic electron flow around PSI (PSI-CEF), chlororespiration, and water-water cycle (5,6). In addition, in cyanobacteria, PQ can be oxidized by terminal oxidases and reduced by respiratory components present at the thylakoid membrane (TM, (7)). PQ-redox is an important element of stress acclimation, regulating state transitions (8,9), synthesis of carotenoids, expression of genes encoding PSII and PSI subunits, proteins from chloroplast and nucleus, superoxide dismutase, and many other enzymes (for a more complete list, see references within the recent works (4,10,11)). Furthermore, PQ-pool redox state plays a key role in mitigating heat stress (12) and salt stress (10,12), acclimation to high light exposure (13) or changing light quality (14,15), and in the establishment of plant response mechanisms to pathogen infection (16). PQ can also have an antioxidant function (17).

PQ-pool redox state can be quantified by HPLC, following the method of Kruk and Karpinski (18). If the PQ/PQH_2 extraction is performed quickly enough to preserve PQ-pool redox state, this method offers fully quantitative analysis, and can discriminate photochemically active PQ within the total PQ pool. With a proper arrangement, it can be used to determine the dependence of the PQ-pool redox state on various experimental/environmental conditions and to follow its shifts, e.g. upon changes in light quality and/or light intensity (11). However, despite all the advantages, this method faces limitations in detecting fast or transient PQ-redox changes. For this reason, optical methods have been developed, based either on light absorbance at 820 nm (19,20) or chlorophyll *a* (Chl *a*) fluorescence (21–24). The absorbance method can detect fast PQ-redox changes upon dark acclimation following illumination. The use of UV-Vis spectrophotometry is basically restricted to investigations in the dark, since no light source is typically connected to these spectrophotometers. All Chl *a* fluorometers, on the other hand, typically include a source of actinic light (AL), making them more applicable in studying light-dependent PQ-redox shifts. The simultaneous measurement of Chl *a* fluorescence and 820 nm transmission has proven effective for detecting light-dependent PQ-redox dynamics (20), however, the need for a combined fluorescence and absorbance measurement setup makes routine adoption of this setup rather limited.

Indeed, the use of Chl *a* fluorescence for PQ-redox monitoring possesses certain limitations. Here, we provide a systematic assessment of the use of fast Chl *a* fluorescence induction, the so-called OJIP

transient (25,26), towards PQ-redox determination under a variety of conditions. The fluorescence transient originates from radiative deactivation of PSII excited state after illumination by a saturation pulse (SP). De-excitation of PSII involves multiple intermediate steps of reduction and oxidation of quinone A (Q_A) and quinone B (Q_B), each characterized by rate constants generally spanning several orders of magnitude, approximately between 10^1 - 10^9 s^{-1} (27). Since the SP length typically ranges between 600 - 2 000 ms, the redox equilibrium within PSII during SP is further influenced by other PETC components. The various phases of the OJIP transient thus reflect kinetic bottlenecks of the electron transport chain (20). In particular, these limitations are the exchange of a reduced PQ molecule to an oxidized one at the Q_B site (J level, at around 2 ms), without involvement of downstream PETCcomponents. The I level (at around 30 ms) represents the limitation in the reoxidation of PQH_2 by the Cyt b_6/f complex. The P level, appearing typically at 200-300 ms in dark-acclimated cells, represents the transient block imposed by inactive FNR, thus it is influenced by the activity of the entire PETC up to the Calvin-Benson-Bassham cycle (CBB) (20,28).

As the most promising parameter for the PQ-redox assessment, the fluorescence yield at the first inflection point J (F_J) has been identified (21). Later on, the normalized F_J value, V_J (Eq. 1), has been recommended as a more precise PQ-redox proxy, since it considers both the initial (F_0) and maximal (F_M) fluorescence yields (22).

In this work, we first examined the applicability of the V_J parameter for assessing PQ-redox state in representative strains of green algae (*Chlorella vulgaris*, *Chlorella* hereafter) and cyanobacteria (*Synechocystis* sp. PCC 6803, *Synechocystis* hereafter) in a dark-acclimated state. Building on these results, we extended the approach to assess PQ-redox under light-acclimated conditions, by defining a novel parameter V_J' (Eq. 2). A systematic comparison of three fluorometers (Multi-Color PAM, AquaPen, and FL 6000; see below for experimental details) showed that both V_J and V_J' parameters can provide information on PQ-redox well in both species when certain preconditions are met. These include fully or at least mostly opened PSII centers (in order to keep the fraction of reduced Q_A^- low), strong SP in order to reduce all Q_A, low culture density to avoid self-shading or fluorescence reabsorption, and correct identification of F_J. The results further indicate higher homeostatic control of the PQ pool redox state in *Synechocystis* compared to *Chlorella*, mainly due to the presence of terminal oxidases (TOs) in/at the thylakoid membranes (7). While acknowledging its specific limitations, the method holds strong potential to become a widely used tool for non-invasive, semi-quantitative PQ-redox determination in algae and cyanobacteria cultures - expanding its application beyond plants, where it has been used exclusively until now.

Methods

Fluorometer settings and V_J calculation

Fast fluorescence induction kinetics (OJIP transients) were measured using a Multi-Color PAM (Walz, Germany), an AquaPen and a FL 6000 fluorometers (Photon System Instruments, Czechia). During the culture density and SP intensity interplay tests, blue (440 - 460 nm) saturation pulse (SP) of intensity 1 100 - 7 500 µmol photons m^{-2} s^{-1} was used for *Chlorella* and red SP (623 - 630 nm) of intensity 975 - 6 500 µmol photons m^{-2} s^{-1} was used for *Synechocystis*. In the other experiments, the SP color and intensity were constant for both *Synechocystis* (625 nm, 1 904 µmol photons m^{-2} s^{-1}) and *Chlorella* (440 nm, 2 244 µmol photons m^{-2} s^{-1}). AquaPen and FL 6000 do not employ a measuring light (ML). In Multi-Color PAM, ML of an intensity < 2 µmol photons m^{-2} s^{-1} was used during SP

application, during acclimation of both *Chlorella* (440 nm ML) and *Synechocystis* (625 nm ML) cultures under AL, as well as ~1 s prior to the SP application in dark-acclimated cultures not treated with DCMU. In the Multi-Color PAM, stirring of the cultures was applied during the whole incubation period, and the stirring was interrupted ~1 s before each OJIP measurement. The OJIP fluorescence recording was initiated 10 ms prior to the SP application. Saturation pulse was applied as a multiple turnover flash, measuring frequency was set to 100 000 Hz. At the onset of SP, the sample-and-hold feature of Multi-Color PAM was applied, in order to suppress signal disturbance by sudden increases in absolute fluorescence intensity. Details of fluorometers settings during all experiments are provided in Supplementary Table S1. The spectra of LEDs used in each fluorometer and in Multi-Cultivator (see below) are shown in Supplementary Figure S1.

To follow the dynamics of the redox state of the PQ pool in fully dark-acclimated cultures, double-normalized OJIP curves were used and the parameter V_J was derived according to previous works (22) :

$$V_J = (F_J - F_O) / (F_M - F_O), \quad (1)$$

where F_J is fluorescence intensity at point J of the OJIP transient (see below for details), F_O is the initial fluorescence yield and F_M is the maximal fluorescence yield. To determine F_J, the fluorescence signal between 0.5 and 5 ms was fitted with a ninth-degree polynomial function. The fitted function's inflection point closest to the expected 2 ms timing was assigned F_J.

To probe PQ-redox in light-acclimated, or partially dark-acclimated cultures, a novel parameter, V_J' was used:

$$V_J' = (F_J' - F_O') / (F_M' - F_O'), \quad (2)$$

where F_O', F_J' and F_M' are the fluorescence intensity at the O and J point of the OJIP transient, and the maximum fluorescence intensity, respectively, measured in light-acclimated or partially dark-acclimated samples. The timing of F_J' was again identified as the inflection point of the reconstructed fluorescence signal closest to 2 ms.

Strains and cultivation conditions

Stock cultures of *Synechocystis* and *Chlorella* were cultivated in Erlenmeyer flasks in BG-11 medium (29,30) at 25°C, under 25 µmol photons m^{-2} s^{-1} of white light in ambient air. For the comparative experiments, both strains were cultivated in Multi-Cultivator MC-1000-MIX (Photon System Instruments, Czechia) in a turbidostat regime. The culture density was maintained between OD_{680} = 0.395 - 0.405, corresponding to ~0.54 and ~0.69 mg Chl *a* L^{-1} for *Synechocystis* and *Chlorella*, respectively. In Multi-Cultivators, the cultures were kept under 25 µmol photons m^{-2} s^{-1} of warm-white LEDs (Supplementary Figure S1), at 25°C, and aeration was secured either by ambient air or by air enriched with CO_2 in a final concentration 0.5% v/v (using Gas Mixing System GMS-150, Photon System Instruments), both provided by at a rate of ~30 mL min^{-1}.

Experimental setup

Comparison of fluorometers under varying culture density and SP intensity

For the density test, cultures were withdrawn from Erlenmeyer flasks, centrifuged (3 000 x*g*, 10 min), and resuspended in fresh BG-11 medium to prepare a series of cultures with concentrations of 0.1 -

24.6 mg Chl *a* L^{-1}. The interplay between culture density and SP intensity was tested by Multi-Color PAM, AquaPen and FL 6000 fluorometers, using dark-acclimated cultures. To avoid detector saturation, OJIP curves were first recorded with the maximal SP intensity in both Multi-Color PAM and FL 6000 fluorometers throughout all culture densities. After the culture density providing the highest signal was identified (3.8 and 2.7 mg Chl *a* L^{-1} for *Synechocystis* and *Chlorella*, respectively; Supplementary Figure S2), detector gain was set such that the fluorescence signal did not exceed 80% of the detector range in these cultures under maximal SP intensity. In the most recent AquaPen version, detector settings cannot be adjusted. All cultures were therefore measured with default settings, leading to detector saturation in many measurements (Fig. 1, Supplementary Figure S2-S3). We note that the only effective strategy to prevent detector saturation in the AquaPen is to either dilute the culture suspension or reduce the saturation pulse intensity, as demonstrated in Fig. 1. Details of fluorometers settings are provided in Supplementary Table S1.

Treatment with DCMU (3-(3,40-dichlorophenyl)-1,1-dimethylurea)

The effect of DCMU was tested on dark-acclimated cultures. After withdrawing cultures from the Multi-Cultivator, aliquots of DCMU stock solution (10 mM, dissolved in DMSO) were added to the 1.5 mL culture aliquots to reach final concentrations 0.1 nM - 20 µM, and then the DCMU-treated samples were dark-acclimated for 20 min. As controls, cultures without DCMU addition were used. To avoid Q_A^- accumulation in PSII prior to the OJIP measurement, the measuring light in Multi-Color PAM was turned off before the OJIP measurements, and it was applied only during SP application.

Dark-to-light transition

During dark-to-light transition experiments, 1.5 mL culture aliquots were withdrawn from the Multi-Cultivator, dark-acclimated for 20 min and transferred to the cuvette of Multi-Color PAM under dim light. Fast fluorescence induction kinetics was measured ~30 s after the transition to the Multi-Color PAM cuvette holder. After the first OJIP measurement, white AL (Supplementary Figure S1) of intensity 100 µmol photons m^{-2} s^{-1} was turned on, and OJIP transients were further measured in 30 s intervals for 5 min. Approximately 1 s before each SP, AL was turned off, and it was resumed right after each OJIP measurement. Measuring light was kept on during the whole measurement course, starting ~5 s before the first OJIP transient recorded in darkness. Multi-Color PAM settings are summarized in Supplementary Table S1. In experiments with added methyl viologen (MV; 98%, Sigma-Aldrich, USA), the cultures were incubated in the presence of MV (final concentration 1 mM and 0.25 mM, 1 M stock solution obtained by dissolving MV in double deionized water) in dark at 25℃ for 20 min prior to the measurements.

Effect of GA, and KCN under illumination

In experiments where the effects of glycolaldehyde (GA; Carl Roth, Germany) and of potassium cyanide (KCN; ≥98%, Sigma-Aldrich, USA) were tested, each inhibitor was added to light-acclimated cultures. After withdrawing from the Multi-Cultivator, 1.5 mL culture aliquots were transferred to the cuvette of Multi-color PAM, to acclimate under white AL (Supplementary Figure S1) of intensity 100 µmol photons m^{-2} s^{-1} for 10 min. OJIP transients were first measured without the presence of inhibitors. Right after this first OJIP measurement, either GA or KCN were added at final concentrations of 25 mM and 1 mM, respectively, and OJIP transients were further measured in 30 s intervals for 5 min under illumination.

High light treatment

During transition from low to high light, 1.5 mL culture aliquots were withdrawn from the Multi-Cultivator, transferred to the cuvette of Multi-color PAM and acclimated under white AL (Supplementary Figure S1) of intensity 25 µmol photons m^{-2} s^{-1} for 5 min. OJIP transients were first measured under 25 µmol photons m^{-2} s^{-1}. Right after the first measurement, AL intensity was increased to 1 500 µmol photons m^{-2} s^{-1} and OJIP curves were further measured in 30 s intervals for 5 min under high light.

Results

Technical aspects of OJIP measurements and correct V_J estimation

Fluorometer selection

In this work, the usability of the fast Chl *a* fluorescence rise (so-called OJIP transient) was tested for the estimation of relative values and changes in the redox state of the PQ pool in *Synechocystis* and *Chlorella*. As a PQ-redox proxy, the normalized value of the fluorescence signal at the J point (V_J, Eq. 1) was selected. The fluorescence induction curves were first recorded using Multi-Color PAM (Heinz Walz GmbH, Germany). This fluorometer uses low-intensity modulated light (so-called measuring light, ML) to induce and monitor fluorescence changes. It can separate fluorescence signal induced by ML from fluorescence induced by actinic light (AL) or SP (31). ML of weak intensity can typically excite only a small fraction of the PSII reaction centers. This is important to mention, since the parameters V_J and V_J' (Eq. 1-2) in fact reflect redox balance within PSII, possibly the ratio of the reduced quinone A (Q_A^-) and quinone B (Q_B) (32,33). The internal PSII redox state can then, with some assumptions (such as 'open' PSII, see below), reflect the redox state of the PQ pool (21). Under normal conditions, where Q_A^- re-oxidation via forward electron transport is not inhibited, the ML effect on the Q_A^-/Q_B equilibrium is negligible. However, the ML can affect PSII redox balance significantly under specific conditions such as in the presence of DCMU (see section 2.2 for details).

In addition to Multi-Color PAM, OJIP transients were also recorded by AquaPen and FL 6000 fluorometers (PSI, Czechia). The principle of fluorescence measurement by Multi-Color PAM is different from these so-called PEA-type, direct fluorometers (named after Handy PEA fluorometer, Hansatech Instruments Ltd, UK (34)) where no ML is used. In these fluorometers, SP is the only light source, the excitation light and the Chl *a* fluorescence are separated using filters, and the measured fluorescence intensity is a function of the SP intensity used. In PEA-type fluorometers, comparing fluorescence traces across SP intensities thus requires initial normalization to SP intensity (35). On the other hand, the absence of ML secures true darkness before the actual Chl *a* fluorescence measurements, resulting in a more precise F_O determination (32).

In addition to the presence of ML, differences between the tested fluorometers include data sampling strategy and detector settings options. Data sampling in Multi-Color PAM is linear across the entire OJIP transient, whereas in both AquaPen and FL 6000 the fluorescence recording is non-linear within specific, predefined intervals. During our fluorometers comparison experiment (Fig. 1, Supplementary Figure S2-S3), the initial 630 ms of OJIP transient was recorded with varying temporal resolution: AquaPen captured 63 data points, FL 6000 captured 827, and Multi-Color PAM captured 63 997 data points. Detector settings, including gain and offset, are accessible only in FL 6000 and Multi-Color PAM. Gain and amplification of the fluorescence signal are common settings for both fluorometers. In FL 6000, offset shifts the signal to lower or even negative voltage values, whereas in Multi-Color

PAM it subtracts background signals. In addition, Multi-Color PAM offers the option to modify the fluorescence detection rate through Frequency and Damping settings. Lowering the measuring frequency can become useful during slow kinetic measurement, however, for OJIP experiments, it is necessary to keep Damping low in order to secure the fastest measuring frequency and highest time resolution possible.

All tested fluorometers provided both blue and red SPs (see Supplementary Figure S1 for details), and detected the fluorescence signal in the red/far red part of the light spectrum (665-750 nm); fluorometers settings and parameters are summarized in Supplementary Table S1. Although the absolute values of the V_J parameter varied slightly among the three tested fluorometers and included some level of noise, the trend of V_J increasing with higher SP intensity and lower culture density was consistent across all fluorometers and in both *Chlorella* and *Synechocystis* cultures (Fig. 1). The primary distinction among the fluorometers was AquaPen's inability to modify detector settings, resulting in detector saturation in many conditions tested, especially in culture suspensions with higher Chl *a* concentration (see the next section for details). Based on our results, Chl *a* concentration below 0.6 mg L^{-1} can be recommended as a safe threshold for avoiding detector saturation when using the AquaPen (Supplementary Figure S2-S3).

Interplay between culture density and saturation pulse intensity

The relative value of F_J depends not only on the redox states of PSII (32) and the PQ pool (21) but also on the intensity of the SP (33,36,37), which is closely related to the density of the liquid suspension culture. To dissect the interplay between SP intensity and culture density, we measured OJIP transients in both *Synechocystis* and *Chlorella* cultures across a density range 0.1 - 24.6 mg Chl *a* L^{-1}, using FL 6000, Multi-Color PAM and AquaPen fluorometers with SP intensities ranging between 975 and 7 500 µmol photons m^{-2} s^{-1} (Supplementary Table S1, Supplementary Figure S2-S3).

In general, V_J was increasing with increasing SP intensity and with decreasing culture density (Fig. 1), consistently with previous works. At low light intensity, the rate of PSII excitation becomes so low that the exchange of an oxidized PQ for a reduced one is not limiting anymore, resulting in no clear J step (33). Such results were also measured here (Supplementary Figure S3, see next section for further details).

Low culture density is generally a prerequisite for Chl *a* fluorescence measurements. In cell suspensions of high density, two key factors potentially affect the fluorescence transients: i) reduced light intensity available for each cell due to self-shading, and ii) reabsorption, or light scattering, of the emitted fluorescence. Both effects are well documented (38,39), and both were reflected in our measurements: absolute fluorescence yields increased from low to moderate culture densities, but declined at higher cell concentrations (Supplementary Figure S2).

Thus, the observed shifts in the V_J parameter across varying SP intensities and culture densities detected by the Multi-Color PAM and FL 6000 fluorometers (Fig. 1) are largely explained by technical aspects of the fluorescence measurement setup, rather than by changes in redox state within PSII or in the PQ pool. At low light intensities, however, determination of V_J can be challenging, as the rate-limiting steps of the photosynthetic electron transport chain become less prominent. To assess PQ-redox from the V_J parameter reliably, the fluorescence measurement requires i) SP of consistent intensity, high enough to secure rapid Q_A^- accumulation and ii) consistent culture density, minimizing self-shading and fluorescence reabsorption.

Determination of the F_J value

The position of F_J in the OJIP transient can be determined in several ways. The traditional and most common method is to detect inflection points of the polyphasic fluorescence rise, with F_J defined as the point typically occurring around 2 ms in dark-acclimated samples (37). Complementary approaches define F_J either as a local minimum in the second derivative of the fluorescence signal around 2 ms (33,40) or as a local maximum in the curvature of the fluorescence rise (41). However, these alternative methods may result in slightly miscalculated both F_J timing and amplitude. From this reason, here both F_J and $F_J^{'}$ were identified as inflection points occurring the most close to the typical timing F_J timing in in dark-acclimated samples, i.e. 2 ms.

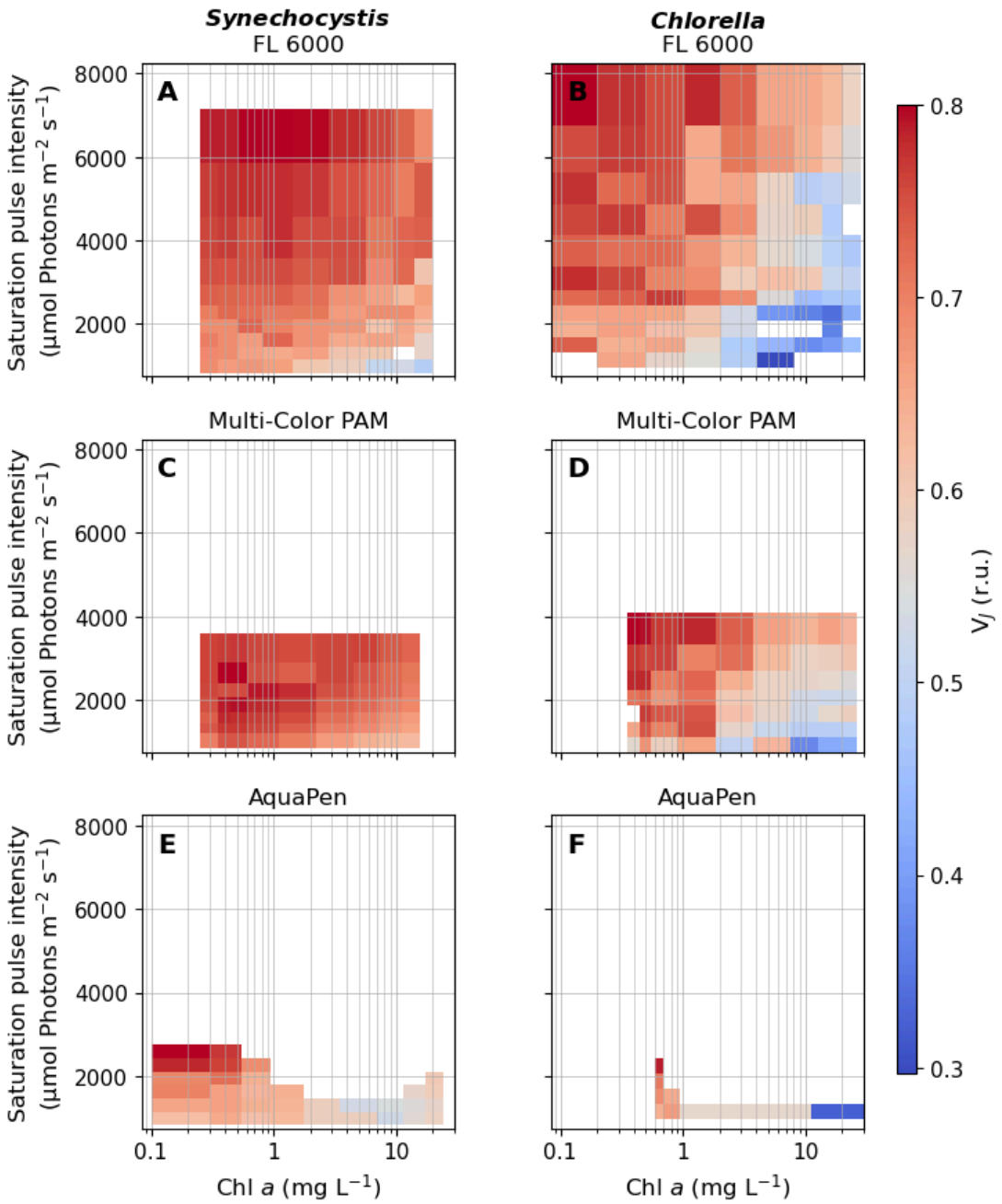

Fig. 1 V_J parameter derived from OJIP transients (summarized in Supplementary Figure S2) measured by FL 6000 (A-B), Multi-Color PAM (C-D) and AquaPen (E-F) fluorometers across a matrix of SP intensity (975 - 7 500 µmol photons m^{-2} s^{-1}) and culture density (0.1 to 24.6 mg Chl *a* L^{-1}) combinations. Before the measurements, *Synechocystis* (A, C, E) and *Chlorella* (B, D, F) cultures were concentrated by centrifugation, diluted with fresh BG-11 medium to final densities and dark-acclimated for 15 - 120 min (see Materials and Methods for details on the experimental setup). The timing of the first step of the fluorescence rise following F_O was determined by identifying inflection points within the 0.6 – 25 ms range, as marked by the grey rectangles in Supplementary Figure S3. For better visualization, the x-axis is shown on a logarithmic scale. Missing values for FL 6000 fluorometer resulted either from high noise under the lowest SP intensities compromising reliable F_J identification, or from finding the first inflection point outside of the specified range. For AquaPen, missing data resulted from detector saturation; when the saturation occurred, the affected OJIP curves were excluded from analysis. A complete description of fluorometers settings, including SP intensities available, is provided in Supplementary Table S1.

V_J shift upon chemical treatments of dark-acclimated cultures

The V_J parameter reflects the level of forward electron transport from PSII. The most straightforward way to demonstrate this effect is to measure OJIP transients in the presence of DCMU (3-(3,40-dichlorophenyl)-1,1-dimethylurea). DCMU binds to the Q_B pocket of PSII and interrupts linear electron flow from PSII to PQ (42). This effect leads to a rapid fluorescence rise along with Q_A^- accumulation (43). When Q_B is displaced from its binding site, even low intensity of ML can lead to significant Q_A reduction. This is due to the much slower rate of Q_A^- recombination with the PSII donor side compared to forward electron transport from Q_A^- to Q_B (27,34). Prior to measuring the DCMU-treated sample, no ML was therefore used.

When the OJIP transients were measured in dark-acclimated *Synechocystis* and *Chlorella* cultures in the presence of 0.1 nM - 20 µM DCMU, the fluorescence rise kinetics became gradually steeper (36,44), as manifested by V_J increase and a loss of the typical I and P steps on the OJIP transient (Fig. 2). At the highest tested DCMU concentration (10-20 µM), only the O-J fluorescence phase was observed, and the fluorescence maximum was reached already at the J step, in line with previous works (45).

Since DCMU inhibits linear electron flow between PSII and PQ, the PQ pool was in fact allowed to become oxidized upon DCMU treatment (46). However, this PQ pool oxidation cannot be detected from Chl *a* fluorescence traces if the PSII reaction centers are closed. To monitor PQ-redox changes upon DCMU treatment, simultaneous measurements of Chl *a* fluorescence and P700 kinetics are required (20,47). The closure of PSII reaction centers in DCMU-inhibited cultures thus compromises the usage of Chl *a* fluorescence alone for PQ-redox estimation.

In control cultures, i.e. without DCMU addition in the dark, V_J level was higher in *Synechocystis* than in *Chlorella* (Fig. 1), suggesting a more reduced PQ pool in *Synechocystis*. This well-studied phenomenon is related to shared components of the photosynthetic and respiratory electron transport chains in cyanobacteria, including the PQ-pool, a central element (48). Respiratory enzymes such as NAD(P)H dehydrogenase-like complex type 1 (NDH-1) or succinate dehydrogenase (SDH) transfer electrons from respiratory metabolism to terminal oxidases (TOs) *via* PQ/PQH_2, causing a partial PQ pool reduction in darkness (49). The cellular organization in cyanobacteria is entirely different from algae or plants where photosynthetic and respiratory apparatus are spatially separated (localized in different organelles) and thus the PQ pool at the thylakoid membrane can become more, or even fully oxidized in darkness (24).

The partially reduced PQ pool in cyanobacteria leads to relatively high F_O (and/or $F_{O'}$) values compared to those of algae or plants (50). This was confirmed here (Supplementary Figure S4-S5). The partially reduced PQ pool forces cyanobacteria to reach State II in darkness, which is characterized by an increased absorption cross-section of PSI (σ_I) and decreased absorption cross-section of PSII (σ_{II}). This ultimately leads to an underestimation of the F_M value, which can only be determined correctly with maximal σ_{II}, i.e. in State I (51). Several methods exist to overcome these limitations and to get true F_O and F_M. For correct F_O determination, pre-illumination by weak far-red or blue light can be used. Such treatment enhances the activity of PSI, which leads to PQ pool oxidation and further induction of State I. However, it should be noted that even with such pre-treatment, F_O will still be overestimated unless corrected for the contribution of fluorescence from PSI and/or free phycobilisomes (PBS) (49,52). For the correct F_M determination, DCMU is often used since it keeps all Q_A reduced (53).

Based on the results of V_J parameter, reaching the maximum value of 1 under DCMU concentrations ≥ 0.1 µM (*Chlorella*) or ≥ 0.01 µM (*Synechocystis*, Fig. 1), such full Q_A reduction and complete PSII closure (possibly involving the induction of PSII conformational changes (54)) was confirmed also here. The increased sensitivity to DCMU in *Synechocystis* was likely related to a more reduced PQ pool in darkness, which led to a more rapid accumulation of Q_A^- during SP application. Another factor influencing observed sensitivity to DCMU can be the different permeability of the inhibitor for various strains and species (55). V_J levels in the presence of DCMU were independent of the carbon saturation level in both *Chlorella* and *Synechocystis* strains (Fig. 1). This fits the expectations: even though the CO_2 level can alter acceptor side limitation of PSI, Y(NA), DCMU makes the fluorescence response insensitive to any changes downstream of PSII. Alongside V_J, also F_O values increased with higher DCMU concentrations (Supplementary Figure S4), as a result of progressive inability to transfer e^- from Q_A to Q_B (27,45).

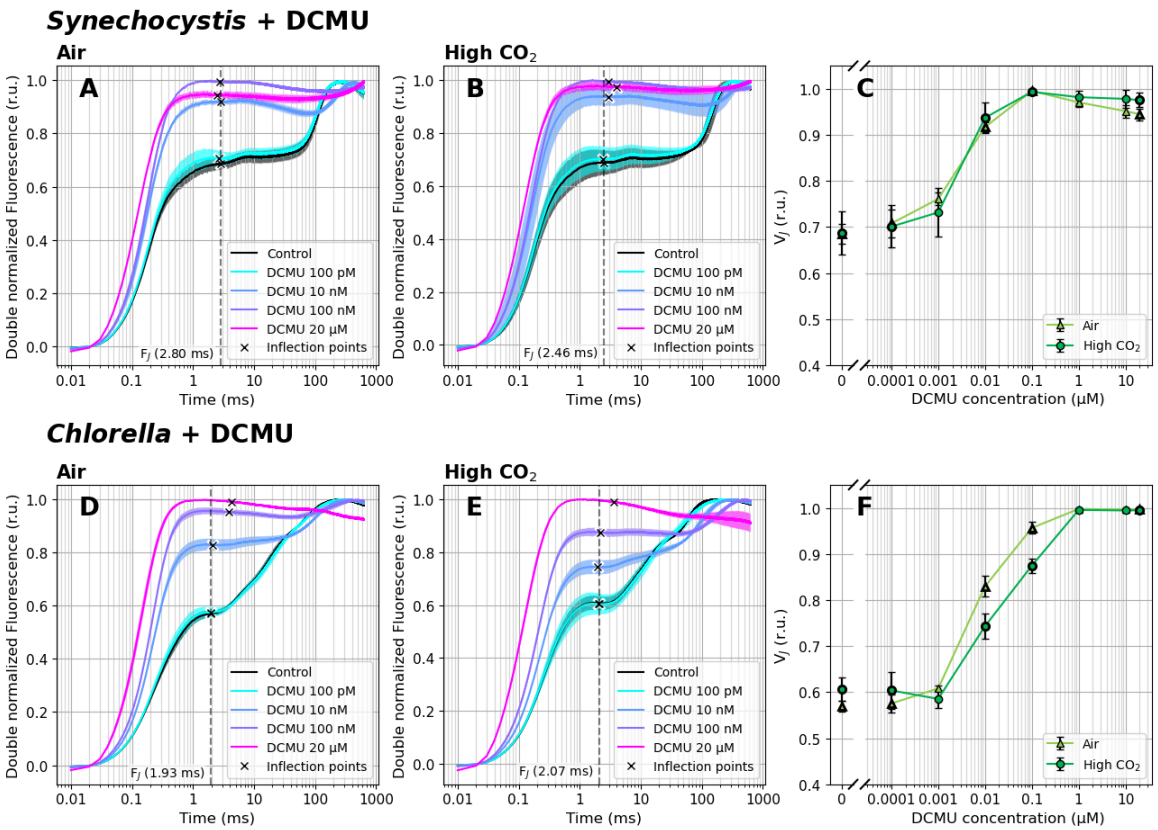

Fig. 2 Fast Chl *a* fluorescence induction kinetics in the presence of 0 - 20 µM DCMU. Cultures of *Synechocystis* (A-C) and *Chlorella* (D-F) were pre-cultivated in a Multi-Cultivator under 25 µmol photons m^{-2} s^{-1} of white light under air (A, D) and 0.5% CO_2 (B, E), and were dark-acclimated for 20 min in the presence of DCMU prior to the fluorescence measurement. After dark acclimation, OJIP curves were recorded using Multi-Color PAM and the parameter V_J (C, F) was calculated according to Eq. (1). OJIP curves in panels A-B and D-E were double normalized between F_O and F_M. The raw OJIP curves are provided in Supplementary Figure S4. F_J timing was identified as the first inflection point of the fluorescence signal around 2 ms, and is marked by crosses in panels A-B and D-E. For simplicity, a single F_J timing (marked by the dashed line) was used for the V_J analysis within each treatment, corresponding with F_J identified in the control culture. Data represent averages ± SD, n = 4.

V_J' dynamics during dark-to-light transition

While Chl *a* fluorescence is not suitable for monitoring PQ-redox under conditions where PSII centers are closed (such as in the presence of DCMU), it has proven to be effective in capturing PQ-redox changes during dark-to-light transition. When the fluorescence rise was measured during dark-to-light transition in the absence of inhibitors, a transient V_J and V_J' increase was found in *Chlorella* cultivated under air (Fig. 3C, F). This was likely related to the delayed activation of ferredoxin-$NADP^+$-oxidoreductase (FNR) and/or Calvin-Benson-Bassham (CBB) cycle upon illumination, which prevented efficient oxidation of PQH_2 by the linear electron transport under actinic light. FNR can be activated within a few seconds (56,57) or in a minute after the dark-to-light transition (58). Enzymes of the CBB cycle get activated during the first minutes of illumination (59). Since CBB is ATP-dependent, formation of a pH gradient across the thylakoid membrane is essential to support CBB operation at a full rate. Previous observations on pH changes in chloroplasts during dark-to-light transitions revealed a stable pH after ~1-2 minutes of illumination both in the thylakoid lumen and the cytoplasm (60). This is roughly consistent with the time of V_J' peak and decline observed in air-cultivated *Chlorella* here (Fig. 3F). After 5 min of illumination, when FNR and CBB get fully activated and NPQ and state transitions form a quasi steady-state, the V_J' value was stabilized, reflecting the light-acclimated state. We note that the timing of V_J' increase, decline and stabilization coincides with the 'slow' Chl *a* fluorescence kinetics measured during dark-to-light transition (34,61).

In *Chlorella* cultivated under high CO_2, V_J' was more stable compared to air-acclimated cultures. Higher CO_2 levels likely resulted in a faster activation of CBB enzymes. Under high CO_2, a greater portion of CBB enzymes (RuBisCO) is located in the chloroplast stroma. Whereas under carbon limitation, key CBB enzymes are found in the pyrenoid, an organelle of carbon-concentrating mechanism (CCM) (62). The CCM secures CO_2 accumulation in the pyrenoid by introducing several diffusion barriers that prevent CO_2 leakage back to the stroma (63). As a result, in high CO_2 conditions, more substrate becomes readily available to RuBisCO which likely minimized FNR and CBB activation time, and mitigated Y(NA) at the onset of illumination.

In *Synechocystis*, the surprisingly stable V_J' during 5 min of illumination was likely a result of the activity of terminal oxidases present in the thylakoid membranes - cytochrome *bd* quinol oxidase (Cyd) and cytochrome *c* oxidase (COX) (64,65). These enzymes can take up electrons from PQH_2, independently of the activation status of FNR and CBB, and therefore prevent PQ pool over-reduction at the onset of illumination. *Synechocystis* can further balance PQ-redox through PBS decoupling and/or state transitions (49). Since F_O' did not decrease, PBS decoupling was unlikely under 100 µmol photons m^{-2} s^{-1} (Supplementary Figure S5). On the other hand, relatively high amount of blue photons in the white AL (about 26% in the range 400-500 nm; Supplementary Figure S1) likely contributed to partial State I induction and partial PQH_2 oxidation under illumination (8), resulting in F_M' increase (Supplementary Fig. S5).

Besides the shifts in V_J', the dark-to-light transition caused shifts in the timing of F_P ("Peak" of the OJIP curve). In the light, F_P' appeared earlier compared to dark in both strains: in *Chlorella* under low and high CO_2, F_P was identified at 115±17 ms and 86±13 ms in dark and at 62±1 ms and 68±0.2 ms after 30 s at light, respectively. In *Synechocystis*, F_P was identified at 333±12 ms and 340±27 ms in dark and at 245±3 ms and 236±6 ms after 30 s at light under low and high CO_2, respectively. The earlier F_P' appearance persisted in *Chlorella*, while in *Synechocystis*, F_P' gradually shifted to a later time over the 5-minute illumination period (353±31 ms and 380±10 ms under low and high CO_2, respectively; Supplementary Figure S5). Earlier appearance of F_P' can be related to an enhanced Y(NA) (66), and/or the activation of the xanthophyll cycle and NPQ (67). During Y(NA), electrons

from PETC cannot be taken up by PSI, which enhances the fluorescence yield of PSII and accelerates OJIP transition. During xanthophyll cycle activation, the pH gradient across the thylakoid membrane gets smaller, which allows Cyt b_6f to transport electrons more efficiently (68). It is also known that the IP phase gets suppressed upon activation of the CBB cycle, leading to earlier appearance of the apparent F_P' (35). Contrary, F_P' can be delayed by an increased pH gradient across the thylakoid membrane which can downregulate the activity of Cyt b_6/f (69), and/or State I→State II transition upon illumination, reducing the amount of light reaching PSII (33).

Indeed, actinic illumination led to Q_A^- accumulation in PSII. In dark-acclimated cells, nearly all PSII reaction centers are in the open state, Q_A is fully oxidized (due to charge recombination with the PSII donor side in the dark), and the oxygen-evolving complex (OEC) is in dark-stable S_1 state (70). Upon illumination by AL of moderate intensity as used here (Fig. 3-6), a portion of P_{680} (the primary electron donor of PSII) gets excited (P_{680}^+), leading to partial reduction of pheophytin ($Pheo^-$) and Q_A (Q_A^-) which further reduced Q_B and form a new redox equilibrium with PQ/PQH_2, depending on state of downstream PETC components. In addition, OEC starts to oscillate through sequential oxidation states ($S_1 \rightarrow S_2 \rightarrow S_3 \rightarrow S_0$), stabilizing likely around S_2 state (70). The OJIP under illumination thus reflected light-driven Q_A^- accumulation in PSII, and the activity of PETC components downstream of PSII influencing PQ-redox.

As a control to the dark-to-light transition experiment, an opposite light-to-dark shift was performed. According to the expectations, V_J' parameter decreased after the transition from light (10 µmol photons m^{-2} s^{-1}) to dark, and the decline was more pronounced in *Chlorella* than in *Synechocystis*. This suggests gradual oxidation of the PQ pool in both strains, and again a more elaborate control of PQ-redox in *Synechocystis*. Full description of the dark-to-light transition experiment is provided in Supplementary material and the results are summarized in Supplementary Figure S6. Taken together, these results confirm that the V_J and V_J' parameters derived from the OJIP curves are sensitive enough to reflect, on a semi-quantitative scale, changes in the redox state of the PQ pool in both dark- and light-acclimated cultures.

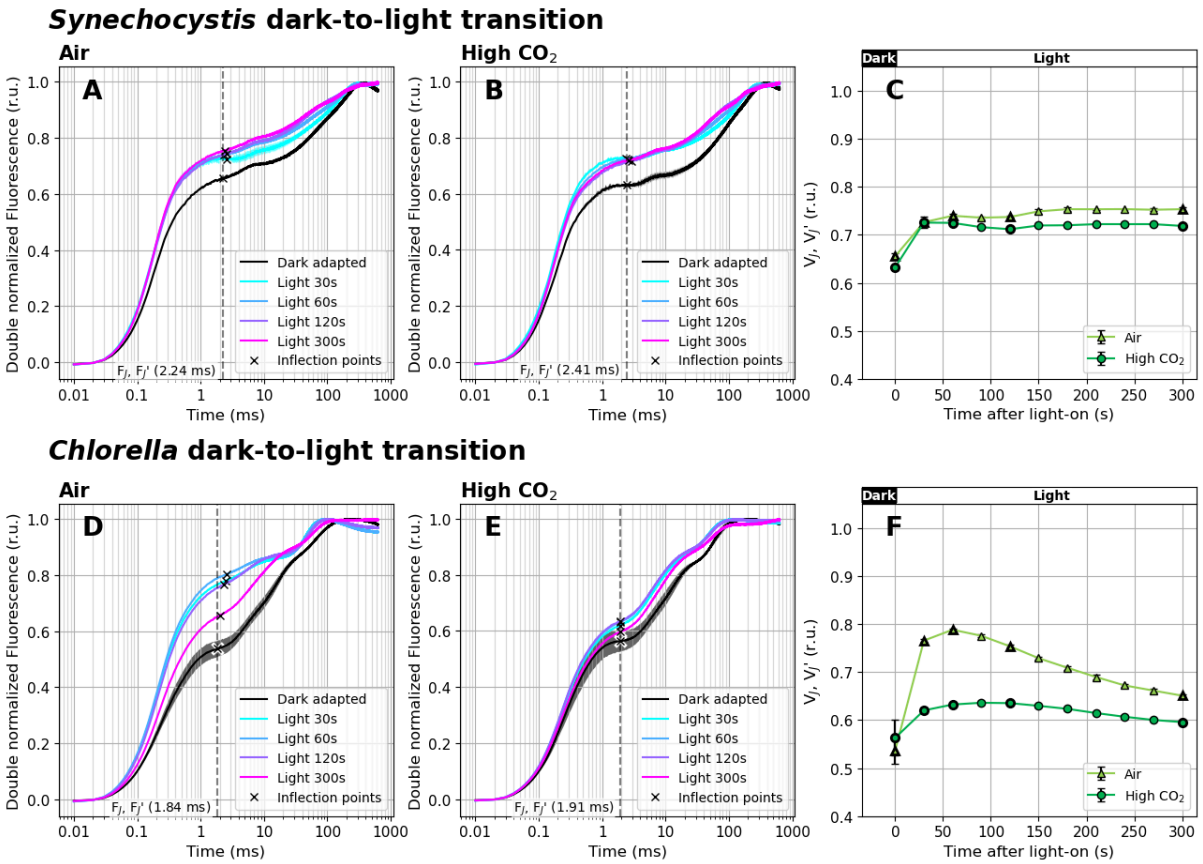

Fig. 3 Fast Chl *a* fluorescence induction kinetics during dark-to-light transition (100 µmol photons m^{-2} s^{-1} of white light). Cultures of *Synechocystis* (A-C) and *Chlorella* (D-F) were pre-cultivated in a Multi-Cultivator under 25 µmol photons m^{-2} s^{-1} of white light under air (A, D) or 0.5% CO_2 (B, E) and were dark-acclimated for 20 min prior to the fluorescence measurement. After dark acclimation, OJIP curves were recorded using Multi-Color PAM and the parameters V_J and V_J' (C, F) were calculated according to Eq. (1) and Eq. (2), respectively. OJIP curves in panels A-B and D-E were double normalized between F_O and F_M (dark-acclimated cultures) or between F_O' and F_M'(light-acclimated cultures). The raw OJIP curves are provided in Supplementary Figure S5. F_J and F_J' timing, identified as the first inflection points of the fluorescence signal around 2 ms, are marked by crosses in panels A-B and D-E. For simplicity, a single F_J' timing was used for V_J' analysis (marked by the dashed line), based on F_J identified in the control culture. Data represent averages ± SD, n = 4.

V_J' dynamics during dark-to-light transition in the presence of methyl viologen

To validate the relationship between the transient V_J increase in air-cultivated *Chlorella* with FNR and CBB activation, OJIP transients during dark-to-light transitions were recorded in the presence of methyl viologen (MV). This chemical efficiently accepts electrons from PSI and FNR and transfers them to molecular oxygen (71,72). It therefore prevents the reduction of $NADP^+$ and cyclic electron flow around PSI, PSI-CEF (73). As described above, illumination of dark-acclimated cells of *Chlorella* resulted in transient V_J' increase due to the inactivity of FNR and/or CBB (Fig. 3F). MV present in 1 mM concentration after 20 min incubation prevented this effect (Fig. 4C,F). At a lower MV concentration (0.25 mM) of MV, the V_J' shift under illumination was less pronounced (Supplementary Figure S7-8).

Interestingly, in dark-acclimated *Chlorella* and *Synechocystis* cultures, the MV presence led to V_J increase, likely due to a reduced IP phase associated with the FNR bypass (Fig. 4, Supplementary Figure S9). This shows a limited capacity of the V_J parameter to efficiently reflect PQ-redox in samples with distinct Y(NA) states. Opposite to previously reported MV treatment in plants (20), we observed a relative increase in the overall OJIP amplitude in both *Chlorella* and *Synechocystis* cultures (when compared to MV-free control, Supplementary Figure S10). Previous studies have shown that when the FNR pathway is fully bypassed, the IP phase disappears entirely (20). In our measurements the IP phase remained detectable in the presence of MV (Supplementary Figure S7-8, S11), albeit reduced compared to control cultures (Supplementary Figure S9-10). The IP phase in *Chlorella* was smaller than previously reported in plants (20), and in *Synechocystis*, it was only barely visible. These results show that a direct comparison of OJIP trends for vascular plants, algae and cyanobacteria needs to be performed with caution. Nevertheless, the 20 min pre-incubation with MV was still long enough to partially prevent Y(NA) at the onset of illumination, as reflected by V_J' reduction (Fig. 4). This confirms that the V_J' parameter is sensitive enough to reflect transient changes in the PQ pool even in actinic light.

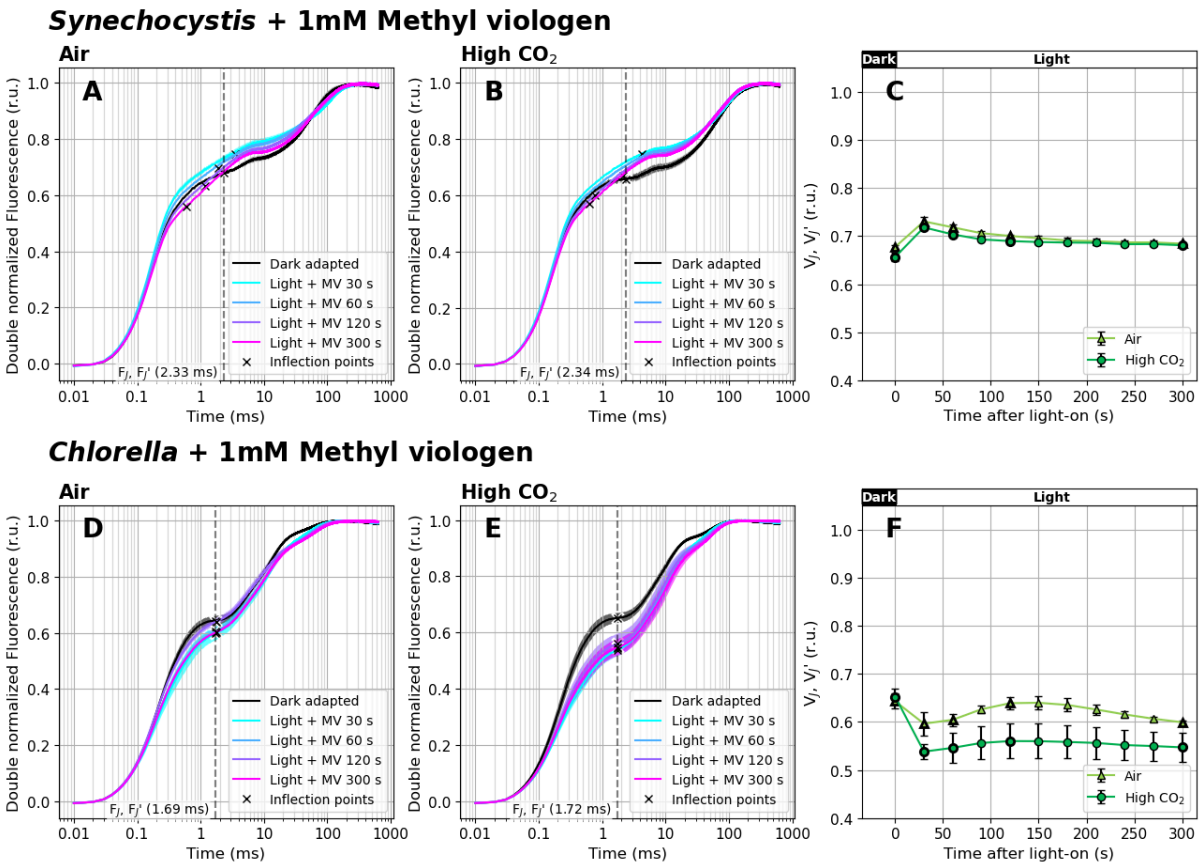

Fig. 4 Fast Chl *a* fluorescence induction kinetics during dark-to-light transition (100 µmol photons m^{-2} s^{-1} of white light) in the presence of 1 mM methyl viologen (MV). Cultures of *Synechocystis* (A-C) and *Chlorella* (D-F) were pre-cultivated in a Multi-Cultivator under 25 µmol photons m^{-2} s^{-1} of white light under air (A, D) or 0.5% CO_2 (B, E) and were dark-acclimated for 20 min prior to the fluorescence measurement in the presence of MV. After dark acclimation, OJIP curves were recorded using Multi-Color PAM and the parameters V_J and V_J' (C, F) were calculated according to Eq. (1) and Eq. (2), respectively. OJIP curves in panels A-B and D-E were double normalized between F_O and F_M. The raw OJIP curves are provided in Supplementary Figure S11. OJIP

curves recorded under 0.25 mM MV are provided in Supplementary Figures S7-S8. F_J and F_J' timing, identified as the first inflection points of the fluorescence signal around 2 ms, are marked by crosses in panels A-B and D-E. For simplicity, a single F_J' timing was used for V_J' analysis (marked by the dashed line), based on F_J identified in the control culture. Data represent averages ± SD, n = 4.

V_J' dynamics upon the addition of glycolaldehyde under illumination

To provide further evidence that the V_J' parameter can reflect changes in PQ-redox under illumination, OJIP curves were further recorded under actinic light in the presence of 25 mM glycolaldehyde (GA). This chemical inhibits enzymes of the CBB cycle (74), and its presence can thus be expected to induce Y(NA) and to increase V_J and V_J' due to PQ pool reduction. Such an assumption was confirmed here. GA was added to the light-acclimated cultures, and it showed an effect already after 30 s of exposure (Fig. 5, Supplementary Fig. S11).

The initial value of V_J', reflecting PQ-redox after 10 min of acclimation to AL of 100 µmol photons m^{-2} s^{-1}, was the highest in *Synechocystis*, lower in *Chlorella* cultivated under air and the lowest in *Chlorella* under high CO_2 (Fig. 5C, F) in accordance with other measurements (Fig. 3, Fig. 6) . The V_J' dynamics after the GA addition was dependent on the CO_2 level under which both *Chlorella* and *Synechocystis* were cultivated. In air-cultivated cultures, V_J was increasing at a higher rate and reached higher levels than in cultures cultivated under high CO_2 (Fig. 5C, F). In *Chlorella*, V_J' reached the maximum value of 1 about 120 s after GA addition, reflecting a highly reduced PQ pool and a lack of alternative routes of PQH_2 oxidation. In high CO_2-cultivated *Chlorella*, the V_J' rise was slower and it stabilized around the value of 0.95, suggesting a slightly less reduced PQ pool compared to low CO_2 conditions. This difference can be attributed simply to higher substrate for CBB being available, and therefore higher GA concentrations needed to fully inhibit the activity of CBB enzymes under high CO_2 conditions. In *Synechocystis*, V_J' shifts were less pronounced than in *Chlorella* (Fig. 5), again likely due to the presence of TOs at thylakoid membrane, balancing PQ reduction upon GA addition.

GA also triggered an increase in F_O' values and changes in F_P' timing (Supplementary Fig. S12). The F_O' increase was likely a result of redox back-pressure on Q_A, similar to the case of DCMU treatment (Supplementary Fig. S4). However, with GA treatment this back-pressure can be expected to originate outside of PSII, in particular in strong Y(NA) that further creates back-pressure on PQH_2. In *Synechocystis*, the F_O' increase was lower compared to *Chlorella*, again likely due to the presence of respiratory enzymes at TM that kept the PQ pool in a more reduced state before the GA treatment, and due to TOs that balanced PQ-redox upon GA application. After 300 s of incubation in the presence of GA, the appearance of F_P' was slightly delayed compared to control in both strains (Supplementary Fig. S12).

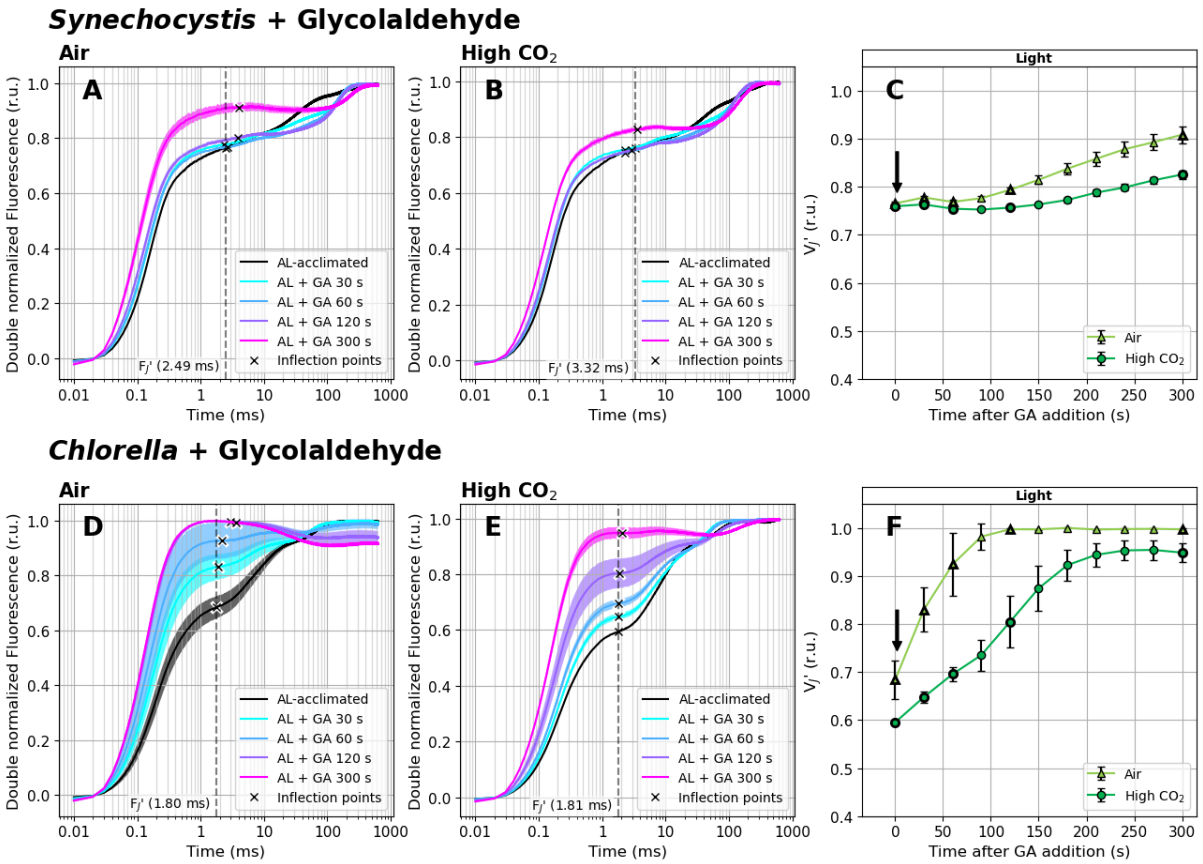

Fig. 5 Fast Chl *a* fluorescence induction kinetics measured under white actinic light (100 µmol photons m^{-2} s^{-1}) in the presence of 25 mM glycolaldehyde (GA). Cultures of *Synechocystis* (A-C) and *Chlorella* (D-F) were pre-cultivated in a Multi-Cultivator under 25 µmol photons m^{-2} s^{-1} of white light under air (A, D) or 0.5% CO_2 (B, E) and were further light-acclimated in the Multi-Color PAM for 10 min prior to the fluorescence measurement under 100 µmol photons m^{-2} s^{-1} of white light. After light acclimation, OJIP curves were recorded using Multi-Color PAM and the parameter V_J' (C, F) was calculated according to Eq. (2). Timing of GA addition, right after the first OJIP measurement, is marked by arrows in panels C and F. OJIP curves in panels A-B and D-E were double normalized between F_O' and F_M'. The raw OJIP curves are provided in Supplementary Figure S12. F_J' timing, identified as the first inflection point of the fluorescence signal around 2 ms, is marked by crosses in panels A-B and D-E. For simplicity, a single F_J' timing (marked by the dashed line) was used for the V_J' analysis within each treatment, corresponding with F_J' identified in the control cultures. Data represent averages ± SD, n = 4.

V_J' dynamics upon addition of KCN under illumination

To confirm that it is indeed the terminal oxidases that balance PQ-redox in *Synechocystis*, OJIP transients were further recorded under actinic light in the presence of 1 mM KCN. This chemical inhibits terminal oxidases such as cytochrome c oxidase (COX) and cytochrome bd quinol oxidase (Cyd), both present in *Synechocystis*, with inhibition constant K_I as low as 7 and 27 µM, respectively (75). It further inhibits the activity of plastocyanin and therefore disrupts linear electron flow between PSII and PSI (76). It may also disrupt the activity of PSII or CBB cycle (77–79), and cause a decrease of pH gradient across the thylakoid membrane (80). Despite such KCN non-specificity, the terminal oxidases are by far the most sensitive KCN targets (75,77,81,82).

Here, KCN was again added to light-acclimated cultures and its effect on the V_J' parameter was evaluated right after addition (in 30 s intervals, for 5 min). This setup prevented the above described unwanted KCN effects on PSII, CBB, plastocyanin or other PETC components during cultures pre-incubation in the KCN presence.

Similar to Fig. 5 and Fig. 3, V_J' after 10 min of acclimation under 100 µmol photons m^{-2} s^{-1}, reflecting PQ-redox in light-acclimated cultures prior to KCN addition, was the highest in *Synechocystis*, lower in *Chlorella* under air and the lowest in *Chlorella* under high CO_2 (Fig. 6C, F). KCN addition induced V_J' increase in both species, and this increase was much faster and more pronounced in *Synechocystis*, where the V_J' reached values of 0.94±0.04 and 0.98±0.01 (high and low CO_2, respectively) already 30 s after KCN addition. In *Chlorella*, V_J' was rising for about 2 min before reaching a stable value around 0.88±0.01 (Fig. 6).

The fast V_J' increase in *Synechocystis* upon KCN addition confirmed the role of both these TOs in PQ-redox balancing. Under AL, PQ is reduced by PSII as well as through metabolism *via* SDH and NDH-1, and oxidized by TOs and PSI. Inactivation of TOs thus creates redox imbalance, which is higher compared to *Chlorella* in which PQ is reduced only by PSII, and oxidized by PSI. In *Synechocystis* cultivated under air, V_J' remained high (0.97±0.03), whereas under high CO_2, the initial rise was only transient and V_J' decreased to 0.76±0.02 after 5 min of illumination (Fig. 6). In *Synechocystis*, the absolute amounts of CBB enzymes and/or terminal oxidases was previously found independent of CO_2 level (83,84). Therefore, the slightly lower and over time decreasing V_J' in *Synechocystis* cultivated under elevated CO_2 was likely a consequence of either more efficient CO_2 fixation simply due to more carbon being available (partially decreasing Y(NA) and further oxidized PQH_2 to a bigger extent compared to low CO_2 condition), or less pronounced e^- flow *via* SDH and NDH-1.

The V_J' increase in *Synechocystis* was accompanied by F_O' rise (Supplementary Figure S13). This is not surprising, as due to the inhibition of TOs by KCN, the ability of PQ to accept e^- from Q_A^- is significantly reduced. This back-pressure on Q_A through PQH_2 led again to Q_A^- accumulation, similarly as upon GA treatment in *Chlorella* (Supplementary Fig. S12). However, in the case of KCN, extra back-pressure on Q_A was likely created by KCN binding to Fe_2^+ of the iron-quinone complex of PSII (79), blocking e^- transport between Q_A and Q_B similar to DCMU (85). In addition, the F_O' value was increasing over the 5 min period in *Chlorella*, whereas it started to decline after 2 min in *Synechocystis*, likely due to a partially induced State I → State II transition (8).

Besides a shift in F_O', a transient dip in the fluorescence induction was recorded between F_J' and F_P' upon KCN addition in *Synechocystis* (Fig. 6A-B). This was likely a consequence of lower affinity of KCN to the enzymes of CBB cycle than to TOs: after impairing TOs, the F_J' fluorescence yield increased (hence, both F_J and V_J became high), however, unlike in the presence of DCMU (Fig. 2) electrons were still able to flow from PQ toward PSI (20) since CBB was not blocked by KCN as strongly as the TOs (77).

In *Chlorella*, V_J' was increasing at a slower rate, and reached lower maximum levels compared to *Synechocystis* (Fig. 6). The only terminal oxidase present in chloroplast of *Chlorella* is plastid terminal oxidase (PTOX), which is, however, resistant to KCN (86). Therefore, the slower V_J' increase in *Chlorella* upon KCN addition, compared to *Synechocystis* (Fig. 4E), was likely reflecting gradual inhibition of plastocyanin and the CBB cycle enzymes (87,88) and gradually impaired electron transport between Q_A and Q_B (we note, however, that PSII inhibition was likely still only

partial after 5 min of measurement in the KCN presence). These effects were again reflected by a dip in the fluorescence induction between F_J' and F_P' (Fig. 6D-E).

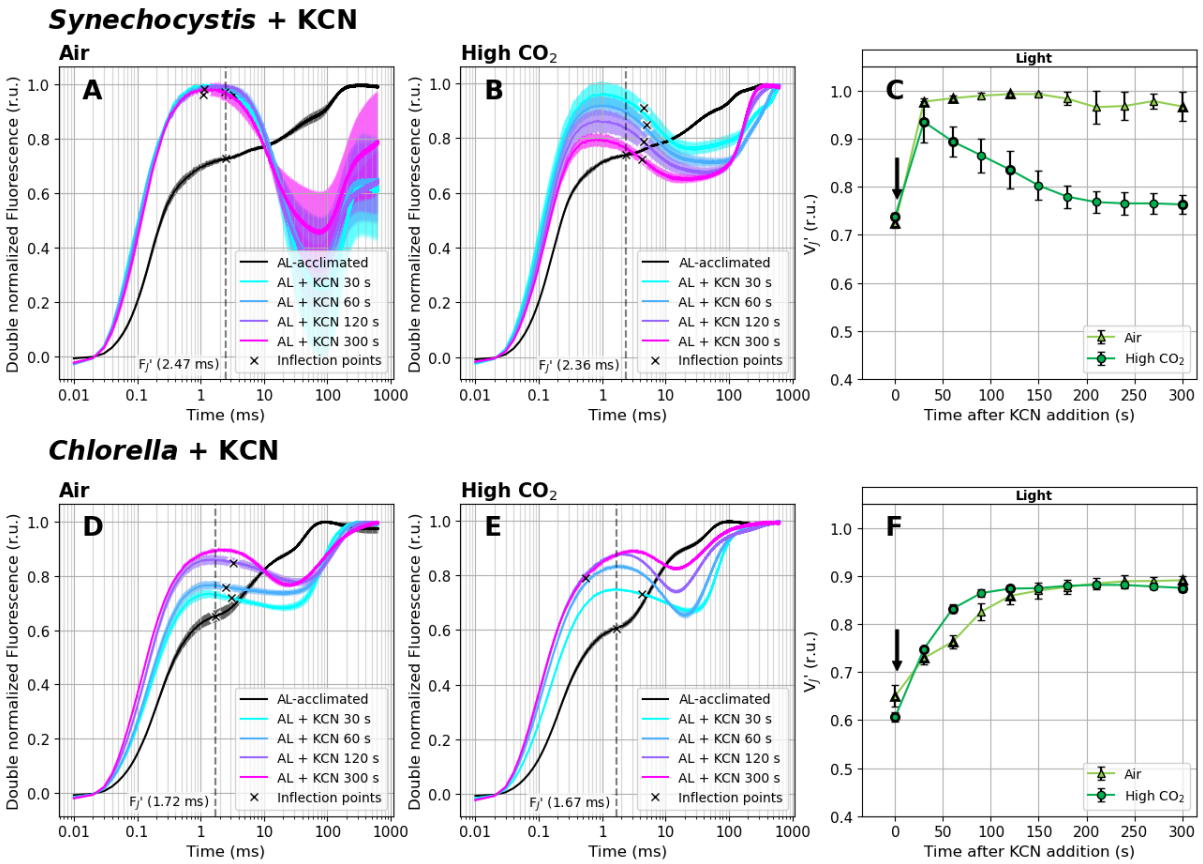

Fig. 6 Fast Chl *a* fluorescence induction kinetics measured under white actinic light (100 µmol photons m^{-2} s^{-1}) in the presence of 1 mM potassium cyanide (KCN). Cultures of *Synechocystis* (A-C) and *Chlorella* (D-F) were pre-cultivated in a Multi-Cultivator under 25 µmol photons m^{-2} s^{-1} of white light under air (A, D) or 0.5% CO_2 (B, E) and were further light-acclimated in the Multi-Color PAM for 10 min prior to the fluorescence measurement under 100 µmol photons m^{-2} s^{-1} of white light. After light acclimation, OJIP curves were recorded using Multi-Color PAM and the parameter V_J' (C, F) was calculated according to Eq. (2). Timing of KCN addition, performed immediately after the first OJIP measurement, is marked by arrows in panels C and F. OJIP curves in panels A-B and D-E were double normalized between F_O' and F_M'. The raw OJIP curves are provided in Supplementary Figure S13. F_J' timing, identified as the first inflection point of the fluorescence signal around 2 ms, is marked by crosses in panels A-B and D-E. For simplicity, a single F_J' timing (marked by the dashed line) was used for the V_J' analysis within each treatment, corresponding with F_J' identified in the controlled culture. Data represent averages ± SD, n = 4.

V_J' shift under high light

Results presented in the previous chapters show that the V_J and V_J' parameters reliably reflect PQ-redox shifts in darkness and under moderate light intensity, but fails to do so under light-induced PSII closure in the presence of DCMU. To provide additional information on the relationship between PSII closure and the ability of the V_J parameter to reflect PQ-redox reliably, we further recorded OJIP

curves during transition from low (25 µmol photons m^{-2} s^{-1}) to high actinic light (HL, 1 500 µmol photons m^{-2} s^{-1}).

Upon high light treatment, the excitation rate of P_{680} increases significantly, leading to higher rate of charge separation within PSII. The excited reaction center of PSII, P_{680}^+ is reduced on the donor side by the redox-active tyrosine residue (Tyr-Z) of the D1 protein, which receives an electron from the oxygen-evolving complex (OEC). Under high light conditions, the OEC is stabilized predominantly in a state close to the S3 intermediate (70). At the acceptor side of PSII, the electrons are transferred through pheophytin to Q_A and Q_B. Since the e^- transport between Q_A and Q_B is several orders of magnitude faster than PQ reduction to PQH_2 (27), Q_A^- accumulates fast upon HL treatment. The OJIP transient, measured in HL-acclimated cultures, is therefore strongly affected by the pre-accumulated Q_A^-. This limits the dynamic range of the fluorescence signal that can reflect changes downstream of PSII, including alterations in PQ-redox. It has been previously shown that after transition from low to high light, the amount of PQH_2 increased from ~0.3 to ~0.75 in *Synechocystis* (as a portion of total PQ pool (46)). Here, the V_J' parameter increased from 0.72±0.03 to 0.8±0.01 in *Synechocystis* (pooled between CO_2 treatments), and from 0.53±0.01 - 0.56±0.01 to 0.73±0.01 - 0.81±0.01 in *Chlorella* under high and low CO_2, respectively (Fig. 7C, F). This clearly demonstrates that under HL, the range of the V_J' parameter reflecting PQ-redox shifts is rather narrow.

Nevertheless, when comparing fluorescence traces after HL treatment in *Synechocystis* and *Chlorella*, differences could be identified, reflecting distinct HL acclimation strategies in both strains. In *Synechocystis*, V_J' increase under HL was less pronounced than in *Chlorella* (Fig. 7), suggesting a better PQ-redox control. This can be again related to the activity of TOs (7), as well as to functional uncoupling of PBS from PSII (89). Such PBS decoupling was measured also here (Supplementary Fig. S14), and it was further reflected in F_O' decrease under HL in *Synechocystis* (Supplementary Fig. S15). Indeed, also decoupled PBS emits fluorescence that might contribute to the overall fluorescence signal, potentially increasing F_O' (90). We note, however, that in *Synechocystis* both PBS decoupling and non-photochemical quenching mediated through orange carotenoid protein (OCP-NPQ) likely dissipated only part of the excessive energy that this strain received under HL (91,92).

Besides these pathways, redox homeostasis can be further balanced by alternative electron flows such as the water-water cycle, cyclic electron flow around PSI (5) or NPQ securing heat dissipation; in *Synechocystis* through OCP-NPQ and in *Chlorella* through the xanthophyll cycle. These protective mechanisms can also lead to a decline of maximal fluorescence value, F_M', as detected in both strains under HL (Supplementary Fig. S15). The F_M' reduction can be further related to gradual PSII damage (93,94), as prolonged limitation of forward electron transport and P_{680}^+ lifetime leads to formation of reactive oxygen species (ROS) both on donor and acceptor sides of PSII (95).

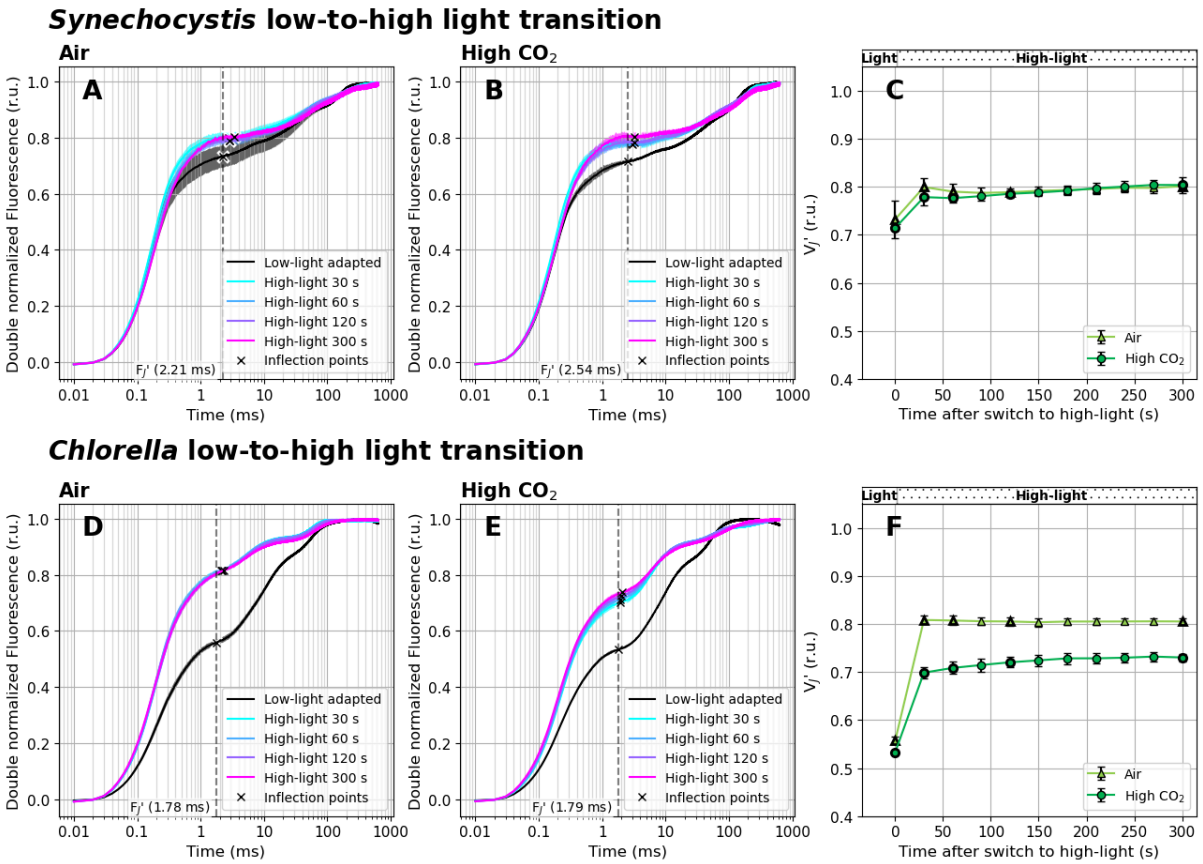

Fig. 7 Fast Chl *a* fluorescence induction kinetics during high light treatment. Cultures of *Synechocystis* (A-C) and *Chlorella* (D-F) were pre-cultivated in a Multi-Cultivator under 25 µmol photons m^{-2} s^{-1} of white light under air (A, D) or 0.5% CO_2 (B, E). Culture aliquotes were transferred to Multi-Color PAM and further acclimated under 25 µmol photons m^{-2} s^{-1} of white light for 5 min. After acclimation, OJIP curves were recorded, the intensity of white light was increased to 1 500 µmol photons m^{-2} s^{-1}, and OJIP curves were further recorded in 30 second intervals for next 5 min. The parameter V_J' (C, F) was calculated according to Eq. (2). OJIP curves in panels A-B and D-E were double normalized between F_O' and F_M'. The raw OJIP curves are provided in Supplementary Figure S15. F_J' timing, identified as the first inflection point of the fluorescence signal around 2 ms, is marked by crosses in panels A-B and D-E. For simplicity, a single F_J' timing (marked by the dashed line) was used for the V_J' analysis within each treatment, corresponding with F_J' identified in the controlled culture. Data represent averages ± SD, n = 4.

Discussion

Advantages of the method

This study evaluates the capacity of fast fluorescence induction kinetics to reflect redox changes in the PQ pool of algae and cyanobacteria. PQ pool is a central element of phototrophic light acclimation and determination of its redox state is often highly desirable. Under defined experimental conditions, the fluorescence method can non-invasively track shifts in the redox state of the PQ pool *in vivo*, provided that key assumptions and limitations are acknowledged (see Discussion). In plant and crop research, it has also been suggested for *in situ* applications (21).

A clear advantage of the method is its simplicity, as no analytical method of PQ/PQH_2 extraction and detection is needed (18,46). The presented method requires 'only' a kinetic fluorometer with high light intensity and high temporal resolution (10^{-6} s, or higher). Such fluorometers are commercially available in many versions and price levels, and can even be built based on open source schemes (96).

The fast Chl *a* fluorescence induction (OJIP) transient is typically measured in a dark-acclimated state, in order to reach a stable, relaxed state of the PETC. This includes relaxation of P_{680}, quasi full oxidation of Q_A and Q_B, oxidation of the PQ-pool to the maximum extent possible under a given conditions, shifting OEC to a dark-stable S_1 state and inactive FNR and CBB-cycle. However, as demonstrated above, the OJIP curves can reflect PQ-redox even in a light-acclimated state. Measuring pre-illuminated cultures, however, prevents correct determination of the true F_O and F_M values that are essential for calculating a variety of parameters (25,28). Nevertheless, the parameter V_J' (Eq. 2) expresses the relative F_J' level with respect to minimal (F_O') and maximal (F_M') fluorescence under the given conditions, providing an estimate of PQ-redox changes in the light-acclimated state. Obtaining true F_O and F_M is especially tricky in cyanobacteria, where F_M is typically measured in the presence of DCMU, while reliable estimation of F_O requires i) a full induction of State I and ii) a correction of the fluorescence signal for contributions from PSI and PBS emission (49,52).

Similarly, the V_J or V_J' parameters can be expected to reflect PQ-redox changes under different SP intensities, as long as the SP is strong enough to induce rapid and complete Q_A^- accumulation , allowing for the appearance of a clear J-step (33). V_J or V_J' can also reflect PQ-redox changes under a variety of culture densities if both self-shading and fluorescence reabsorption within the cell culture are negligible (38,39).

Limitations of the method

While useful, the use of the V_J and V_J' parameters as a proxy for PQ-redox assessment comes with certain limitations. The most critical requirement is to ensure identical sample pre-treatment. In addition to pre-illumination or the presence of inhibitors (Fig. 1-5), this also includes temperature.

The method has several ultimate limits. First, the method fails when the accumulation of Q_A^- does not reflect shifts in PQ-redox. This can be best illustrated by the examples of strong V_J increase under DCMU treatment (Fig. 2) and, on the contrary, only a little V_J' increase under high light treatment (Fig. 7) not reflecting strong PQ reduction (18,46). The OJIP measurements during transition from low to high light show that the more Q_A^- is accumulated in PSII prior to the OJIP curve measurement, the less oxidized Q_A remains available to form equilibrium with PETC components downstream of PSII, including PQ/PQH_2. Second, considering the way of how V_J' is calculated (using F_O' and F_M' values), it is clear that the working range of this parameter is strongly reduced compared to the parameter V_J. When F_J' gets higher than F_P', e.g. upon GA (Fig. 5) or KCN addition (Fig. 6), V_J' can rise only up to the value of 1. The question whether in such state, 100% of the photoactive PQ pool - which accounted for approximately 30-50% of total PQ pool in previous studies (18,46) - is fully reduced to PQH_2 remains to be resolved. Similarly, it is still unclear whether the size of the photoactive PQ pool changes under these or other chemical treatments.

Furthermore, in our experiments using Multi-Color PAM with a 725 nm LED, pretreatment of fully dark-acclimated cultures with far-red light never reduced V_J below the value of 0.46 in *Chlorella* and 0.61 in *Synechocystis* (data not shown). This contrasts with previous studies, which reported that only

approximately 20–30% of the photoactive PQ pool was reduced in *Synechocystis* cultures (46) or *Arabidopsis thaliana* leaves under far-red light (18). The method thus reflects trends in relative PQ-redox changes but not absolute PQ/PQH_2 amounts.

Lessons towards understanding PQ pool homeostasis in algae and cyanobacteria

Our results show that *Synechocystis* keeps impressively tight control over PQ-redox across a wide range of conditions, including dark-to-light or low-to-high light transitions, compared to *Chlorella*. This is in full agreement with previous works (97). The PQ pool becomes reduced either by exposure to high light, or upon cultivation under red light, even of very low intensity (14,98). To cope with high light under long-term exposure, *Synechocystis* adopted several acclimation mechanisms such as reduction of the light-harvesting antenna and abundance of PETC components (83), shifts in the PSII/PSI ratio (99) or an increase of intracellular glycogen (100), lipid and/or carotenoids (101). These strategies contribute to adjusting light energy distribution between photosystems, balancing PQ-redox and ATP to NADPH ratio (102). At the onset of high light exposure, the most important factor for maintaining PQ-redox homeostasis, in addition to decoupling PBS and activation of OCP-NPQ, is the activity of TOs (7,103). Indeed, also increased concentration of CO_2 helps to prevent PQ-pool overeduction upon high light exposure (46).

Even though *Chlorella* possesses PTOX in its chloroplasts, it appears less effective in regulating PQ-redox compared to *Synechocystis*. Under the conditions of high energy inflow, increased PETC activity is accompanied by the build up of a high pH gradient across the thylakoid membrane, resulting in acidification of the thylakoid lumen. Lowering the lumenal pH induces xanthophyll cycle and NPQ, which, together with State I → State II transition, downregulates the amount of energy exciting P_{680} and reducing Q_A. The pH level in chloroplasts is under homeostatic control, which is however still to be fully understood (104). The pH homeostasis in chloroplasts also contributes to the long-term regulation of PQ redox balance. However, as shown also here, upon sudden shifts in light intensity, PQ-redox can face rapid changes since algae (similar to plants) have only limited options of its control.

Conclusions

In this study, we critically assess the use of fast Chl *a* fluorescence rise kinetics (OJIP transients) as an indicator of the redox state of the plastoquinone pool (PQ-redox) in liquid cultures of algae and cyanobacteria. We show that with certain limitations, the method is sensitive enough to detect relative PQ-redox changes in both dark- and light-acclimated *Chlorella* and *Synechocystis* cells, using V_J and V_J' parameters (Eq. 1 and 2, respectively). The method requires 1) sufficiently intense saturation pulses (SP) to induce rapid Q_A^- accumulation; 2) relatively low culture density to prevent self-shading and fluorescence reabsorption; 3) similar rates of Q_A^- accumulation in the control and treated samples and 4) appropriate electron flow between Q_A^-, Q_B and PQ. The V_J parameter reflects the PQ-redox best in dark-acclimated cultures. Under low to moderate actinic light, the V_J' parameter is still able to reflect PQ-redox changes, however, not as reliably as in the dark. This is because part of Q_A gets reduced to Q_A^- even before a saturation pulse is applied to induce the OJIP transient, resulting in less Q_A being able to form equilibrium with plastoquinone upon SP application. This implies that the V_J or V_J' range, reflecting PQ-redox, strongly depends on the culture pre-treatment. Nevertheless, even under 100 µmol photons m^{-2} s^{-1} of white light, the V_J' parameter effectively reflected strong PQ pool reduction, as induced by GA and KCN in light-acclimated *Chlorella* and *Synechocystis* cultures,

respectively. This also implies that for F_J' normalization, true F_O and F_M is not needed, and the values of F_O' and F_M' are sufficient. Even though only semi-quantitative, the fluorescence method provides an easy-to-use alternative to traditional HPLC-based approaches for detecting relative PQ-redox shifts. The method, being fast and non-invasive, has a great potential to become widely used in algae and cyanobacteria research, in addition to plant research where it is already well established.

List of abbreviations:

AL - actinic light; **CBB** - Calvin-Benson-Bassham cycle; **COX** - cytochrome *c* oxidase; **Cyt b_6/f** - Cytochrome b_6/f; **Cyd** - cytochrome *bd* quinol oxidase; **DCMU** - 3-(3,40-dichlorophenyl)-1,1-dimethylurea; **F_O**, **F_O'**- initial fluorescence yield at the beginning of the OJIP curve in fully dark-acclimated samples (≥ 20 min in darkness) and in light-acclimated or partially dark-acclimated samples, respectively; **F_I**, **F_J** and **F_P** - fluorescence yield at the J, I and P point of the OJIP curve in fully dark-acclimated cells (≥ 20 min in darkness), respectively; **F_I'**, **F_J'** and **F_P'** - fluorescence yield at the J, I and P point of the OJIP curve in light- or partially dark-aclimated cells, respectively; **F_M, F_M'** - maximal fluorescence yield in fully dark-acclimated cells (≥ 20 min in darkness) and in light-acclimated or partially dark-acclimated samples, respectively; **FNR** - ferredoxin-$NADP^+$-oxidoreductase; **GA** - glycolaldehyde; **HL** - high light; **J**, **I**, **P** - J, I and P points of the OJIP curve, respectively; **ML** - measuring light; **MV** - methyl viologen; **NDH-1** - NAD(P)H dehydrogenase-like complex type 1; **NPQ** - non-photochemical quenching; **OEC** - oxygen evolving complex of PSII, **OCP** - orange carotenoid protein; **PBS** - phycobilisomes; **PC** - plastocyanin; **PQ** - plastoquinone; **PQH_2** - plastoquinol; **PQ-redox** - redox state of the PQ/PQH_2 pool; **PETC** - photosynthetic electron transport chain; **PSI** - Photosystem I; **PSI-CEF** - cyclic electron flow around PSI; **PSII** - Photosystem II; **PTOX** - plastid terminal oxidase; **Q_A** - quinone A; **Q_B** - quinone B; **SDH** - succinate dehydrogenase; **SP** - saturating pulse; **TOs** - terminal oxidases; **V_J**, **V_J'**- relative fluorescence yield at the J point of the OJIP curve measured in fully dark-acclimated and in partially dark- or light-acclimated samples, respectively; **Y(NA)** - acceptor side limitation of PSI

Ethics approval and consent to participate

Not applicable

Consent for publication

Not applicable

Availability of data and materials

The datasets generated during and/or analysed during the current study are available in the Figshare repository under DOI 10.6084/m9.figshare.28938632. The python scripts created and used to evaluate the measured OJIP curves can be accessed at https://github.com/Computational-Biology-Aachen/OJIP-PQredox. The repository includes a Jupyter notebook (paper_figures.ipynb) that reproduces all figures in the manuscript. Additionally, we provide a freely accessible online tool for streamlined processing and preliminary analysis of OJIP fluorescence data from the three fluorometers evaluated in this study, available at https://tools-py.e-cyanobacterium.org/.

Competing interests

The authors declare that they have no competing interests

Funding

This work was supported by the Ministry of Education, Youth and Sports of CR (LUAUS24149), by the National Research, Development and Innovation Office (RRF-2.3.1-21-2022-00014), and Deutsche Forschungsgemeinschaft (DFG, German Research Foundation) under Germany's Excellence Strategy—EXC-2048/1.

Authors' contributions

TZ, AChP and TP designed and planned the research, performed the experiments and evaluated the data, TZ wrote the manuscript with contributions from all authors. All authors reviewed, revised and approved the final manuscript for publication.

Acknowledgements

Not applicable

References

1. Nelson N, Yocum CF. Structure and function of photosystems I and II. Annu Rev Plant Biol. 2006;57:521–65.

2. Li H, Nakajima Y, Nango E, Owada S, Yamada D, Hashimoto K, et al. Oxygen-evolving photosystem II structures during S-S-S transitions. Nature. 2024 Feb;626(7999):670–7.

3. Blankenship RE. Molecular mechanisms of photosynthesis. Blankenship RE, editor. Oxford, UK: Wiley; 2002.

4. Havaux M. Plastoquinone In and Beyond Photosynthesis. Trends Plant Sci. 2020 Dec;25(12):1252–65.

5. Miyake C. Alternative electron flows (water-water cycle and cyclic electron flow around PSI) in photosynthesis: molecular mechanisms and physiological functions. Plant Cell Physiol. 2010 Dec;51(12):1951–63.

6. Bernát G, Rögner M. Center of the Cyanobacterial Electron Transport Network: The Cytochrome b 6 f Complex. In: Bioenergetic Processes of Cyanobacteria. Dordrecht: Springer Netherlands; 2011. p. 573–606.

7. Lea-Smith DJ, Ross N, Zori M, Bendall DS, Dennis JS, Scott SA, et al. Thylakoid terminal oxidases are essential for the cyanobacterium Synechocystis sp. PCC 6803 to survive rapidly changing light intensities. Plant Physiol. 2013 May;162(1):484–95.

8. Calzadilla PI, Kirilovsky D. Revisiting cyanobacterial state transitions. Photochem Photobiol Sci. 2020 May 1;19(5):585–603.

9. Virtanen O, Tyystjärvi E. Plastoquinone pool redox state and control of state transitions in Chlamydomonas reinhardtii in darkness and under illumination. Photosynth Res. 2023

Jan;155(1):59–76.

10. Pilarska M, Niewiadomska E, Kruk J. Salinity-induced changes in plastoquinone pool redox state in halophytic Mesembryanthemum crystallinum L. Sci Rep. 2023 Jul 10;13(1):11160.

11. Mattila H, Khorobrykh S, Hakala-Yatkin M, Havurinne V, Kuusisto I, Antal T, et al. Action spectrum of the redox state of the plastoquinone pool defines its function in plant acclimation. Plant J. 2020 Nov 1;104(4):1088–104.

12. Pshybytko NL, Kruk J, Kabashnikova LF, Strzalka K. Function of plastoquinone in heat stress reactions of plants. Biochim Biophys Acta. 2008 Nov;1777(11):1393–9.

13. Lepetit B, Sturm S, Rogato A, Gruber A, Sachse M, Falciatore A, et al. High light acclimation in the secondary plastids containing diatom Phaeodactylum tricornutum is triggered by the redox state of the plastoquinone pool. Plant Physiol. 2013 Feb;161(2):853–65.

14. Zavřel T, Segečová A, Kovács L, Lukeš M, Novák Z, Pohland AC, et al. A Comprehensive Study of Light Quality Acclimation in Synechocystis Sp. PCC 6803. Plant Cell Physiol [Internet]. 2024 May 28; Available from: http://dx.doi.org/10.1093/pcp/pcae062

15. Bernát G, Zavřel T, Kotabová E, Kovács L, Steinbach G, Vörös L, et al. Photomorphogenesis in the Picocyanobacterium Includes Increased Phycobilisome Abundance Under Blue Light, Phycobilisome Decoupling Under Near Far-Red Light, and Wavelength-Specific Photoprotective Strategies. Front Plant Sci. 2021 Mar 18;12:612302.

16. Nosek M, Kornaś A, Kuźniak E, Miszalski Z. Plastoquinone redox state modifies plant response to pathogen. Plant Physiol Biochem. 2015 Nov;96:163–70.

17. Khorobrykh S, Tyystjärvi E. Plastoquinol generates and scavenges reactive oxygen species in organic solvent: Potential relevance for thylakoids. Biochim Biophys Acta Bioenerg. 2018 Oct;1859(10):1119–31.

18. Kruk J, Karpinski S. An HPLC-based method of estimation of the total redox state of plastoquinone in chloroplasts, the size of the photochemically active plastoquinone-pool and its redox state in thylakoids of Arabidopsis. Biochim Biophys Acta. 2006 Dec;1757(12):1669–75.

19. Ivanov B, Mubarakshina M, Khorobrykh S. Kinetics of the plastoquinone pool oxidation following illumination Oxygen incorporation into photosynthetic electron transport chain. FEBS Lett. 2007 Apr 3;581(7):1342–6.

20. Schansker G, Tóth SZ, Strasser RJ. Methylviologen and dibromothymoquinone treatments of pea leaves reveal the role of photosystem I in the Chl a fluorescence rise OJIP. Biochim Biophys Acta. 2005 Feb 17;1706(3):250–61.

21. Tóth SZ, Schansker G, Strasser RJ. A non-invasive assay of the plastoquinone pool redox state based on the OJIP-transient. Photosynth Res. 2007 May 9;93(1-3):193–203.

22. Tsimilli-Michael M, Stamatakis K, Papageorgiou GC. Dark-to-light transition in Synechococcus sp. PCC 7942 cells studied by fluorescence kinetics assesses plastoquinone redox poise in the dark and photosystem II fluorescence component and dynamics during state 2 to state 1 transition. Photosynth Res. 2009 Mar;99(3):243–55.

23. Fukunaga T, Ogawa T, Iwasaki W, Sonoike K. Phylogenetic Profiling Analysis of the Phycobilisome Revealed a Novel State-Transition Regulator Gene in Synechocystis sp. PCC 6803. Plant Cell Physiol [Internet]. 2024 Jul 22; Available from: http://dx.doi.org/10.1093/pcp/pcae083

24. Naydov I, Kozuleva M, Ivanov B, Borisova-Mubarakshina M, Vilyanen D. Pathways of Oxygen-Dependent Oxidation of the Plastoquinone Pool in the Dark After Illumination. Plants (Basel) [Internet]. 2024 Dec 12;13(24). Available from: http://dx.doi.org/10.3390/plants13243479

25. Stirbet A, Lazár D, Kromdijk J, Govindjee G. Chlorophyll a fluorescence induction: Can just a one-second measurement be used to quantify abiotic stress responses? Photosynthetica. 2018 Mar 1;56(SPECIAL ISSUE):86–104.

26. Strasser RJ, Govindjee. The fo and the O-J-I-P fluorescence rise in higher plants and algae. In: Regulation of Chloroplast Biogenesis. Boston, MA: Springer US; 1992. p. 423–6.

27. Lazár D. Chlorophyll a fluorescence rise induced by high light illumination of dark-adapted plant tissue studied by means of a model of photosystem II and considering photosystem II heterogeneity. J Theor Biol. 2003 Feb 21;220(4):469–503.

28. Tsimilli-Michael M. Special issue in honour of Prof. Reto J. Strasser - Revisiting JIP-test: An educative review on concepts, assumptions, approximations, definitions and terminology. Photosynthetica. 2020 May 28;58(SPECIAL ISSUE):275–92.

29. Rippka R, Stanier RY, Deruelles J, Herdman M, Waterbury JB. Generic assignments, strain histories and properties of pure cultures of Cyanobacteria. Microbiology. 1979 Mar 1;111(1):1–61.

30. van Alphen P, Abedini Najafabadi H, Branco Dos Santos F, Hellingwerf KJ. Increasing the Photoautotrophic Growth Rate of Synechocystis sp. PCC 6803 by Identifying the Limitations of Its Cultivation. Biotechnol J. 2018 Aug;13(8):e1700764.

31. Schreiber U. Detection of rapid induction kinetics with a new type of high-frequency modulated chlorophyll fluorometer. Photosynth Res. 1986 Jan;9(1-2):261–72.

32. Schansker G, Strasser RJ. Quantification of non-QB-reducing centers in leaves using a far-red pre-illumination. Photosynth Res. 2005 Jun;84(1-3):145–51.

33. Tomek P, Lazár D, Ilík P, Naus J. Research note: On the intermediate steps between the O and P steps in chlorophyll a fluorescence rise measured at different intensities of exciting light. Funct Plant Biol. 2001;28(11):1151.

34. Kalaji HM, Schansker G, Ladle RJ, Goltsev V, Bosa K, Allakhverdiev SI, et al. Frequently asked questions about in vivo chlorophyll fluorescence: practical issues. Photosynth Res. 2014 Nov;122(2):121–58.

35. Schansker G, Tóth SZ, Strasser RJ. Dark recovery of the Chl a fluorescence transient (OJIP) after light adaptation: the qT-component of non-photochemical quenching is related to an activated photosystem I acceptor side. Biochim Biophys Acta. 2006 Jul;1757(7):787–97.

36. Schansker G, Tóth SZ, Kovács L, Holzwarth AR, Garab G. Evidence for a fluorescence yield change driven by a light-induced conformational change within photosystem II during the fast chlorophyll a fluorescence rise. Biochim Biophys Acta. 2011 Sep;1807(9):1032–43.

37. Strasserf RJ, Srivastava A, Govindjee. POLYPHASIC CHLOROPHYLL *a* FLUORESCENCE TRANSIENT IN PLANTS AND CYANOBACTERIA. Photochem Photobiol. 1995 Jan;61(1):32–42.

38. Kumar Panigrahi S, Kumar Mishra A. Inner filter effect in fluorescence spectroscopy: As a problem and as a solution. J Photochem Photobiol C: Photochem Rev. 2019 Dec;41(100318):100318.

39. Du W, Jongbloets JA, Pineda Hernández H, Bruggeman FJ, Hellingwerf KJ, Branco dos Santos F. Photonfluxostat: A method for light-limited batch cultivation of cyanobacteria at different, yet constant, growth rates. Algal Res. 2016 Dec;20:118–25.

40. Akinyemi OO, Čepl J, Keski-Saari S, Tomášková I, Stejskal J, Kontunen-Soppela S, et al. Derivative-based time-adjusted analysis of diurnal and within-tree variation in the OJIP fluorescence transient of silver birch. Photosynth Res. 2023 Sep;157(2-3):133–46.

41. Xia Q, Tan J, Cheng S, Jiang Y, Guo Y. Sensing Plant Physiology and Environmental Stress by Automatically Tracking F and F Features in PSII Chlorophyll Fluorescence Induction. Photochem Photobiol. 2019 Nov;95(6):1495–503.

42. Velthuys BR. Electron‐dependent competition between plastoquinone and inhibitors for binding to photosystem II. FEBS Lett. 1981 Apr 20;126(2):277–81.

43. Schreiber U, Schliwa U, Bilger W. Continuous recording of photochemical and non-photochemical chlorophyll fluorescence quenching with a new type of modulation fluorometer. Photosynth Res. 1986 Jan;10(1-2):51–62.

44. Schansker G, Tóth SZ, Holzwarth AR, Garab G. Chlorophyll a fluorescence: beyond the limits of the Q(A) model. Photosynth Res. 2014 May;120(1-2):43–58.

45. Tóth SZ, Schansker G, Strasser RJ. In intact leaves, the maximum fluorescence level (F(M)) is independent of the redox state of the plastoquinone pool: a DCMU-inhibition study. Biochim Biophys Acta. 2005 Jun 30;1708(2):275–82.

46. Khorobrykh S, Tsurumaki T, Tanaka K, Tyystjärvi T, Tyystjärvi E. Measurement of the redox state of the plastoquinone pool in cyanobacteria. FEBS Lett. 2020 Jan;594(2):367–75.

47. Belyaeva NE, Bulychev AA, Riznichenko GY, Rubin AB. Thylakoid membrane model of the Chl a fluorescence transient and P700 induction kinetics in plant leaves. Photosynth Res. 2016 Dec;130(1-3):491–515.

48. Vermaas WFJ. Photosynthesis and Respiration in Cyanobacteria. In: Encyclopedia of Life Sciences [Internet]. Chichester, UK: John Wiley & Sons, Ltd; 2001. Available from: https://onlinelibrary.wiley.com/doi/10.1038/npg.els.0001670

49. Stirbet A, Lazár D, Papageorgiou GC, Govindjee. Chlorophyll a fluorescence in Cyanobacteria: Relation to photosynthesis. In: Cyanobacteria. Elsevier; 2019. p. 79–130.

50. Campbell D, Hurry V, Clarke AK, Gustafsson P, Oquist G. Chlorophyll fluorescence analysis of cyanobacterial photosynthesis and acclimation. Microbiol Mol Biol Rev. 1998 Sep;62(3):667–83.

51. Bhatti AF, Kirilovsky D, van Amerongen H, Wientjes E. State transitions and photosystems spatially resolved in individual cells of the cyanobacterium Synechococcus elongatus. Plant Physiol. 2021 May 27;186(1):569–80.

52. Ogawa T, Sonoike K. Effects of Bleaching by Nitrogen Deficiency on the Quantum Yield of Photosystem II in Synechocystis sp. PCC 6803 Revealed by Chl Fluorescence Measurements. Plant Cell Physiol. 2016 Mar;57(3):558–67.

53. Campbell D, Oquist G. Predicting Light Acclimation in Cyanobacteria from Nonphotochemical Quenching of Photosystem II Fluorescence, Which Reflects State Transitions in These Organisms. Plant Physiol. 1996 Aug;111(4):1293–8.

54. Sipka GB, Magyar M, Mezzetti A, Akhtar P, Zhu Q, Xiao Y, et al. Light-adapted charge-separated state of photosystem II: structural and functional dynamics of the closed

reaction center. Plant Cell. 2021 May 31;33(4):1286–302.

55. Senger H. Changes in the sensitivity to inhibitors of photosynthesis during the life cycle of unicellular algae. Plant and Cell Physiology. 1977;17:229–38.

56. Kramer M, Rodriguez-Heredia M, Saccon F, Mosebach L, Twachtmann M, Krieger-Liszkay A, et al. Regulation of photosynthetic electron flow on dark to light transition by ferredoxin:NADP(H) oxidoreductase interactions. Elife [Internet]. 2021 Mar 9;10. Available from: http://dx.doi.org/10.7554/eLife.56088

57. Nikkanen L, Toivola J, Trotta A, Diaz MG, Tikkanen M, Aro EM, et al. Regulation of cyclic electron flow by chloroplast NADPH-dependent thioredoxin system. Plant Direct. 2018 Nov;2(11):e00093.

58. Harbinson J, Hedley CL. Changes in P-700 Oxidation during the Early Stages of the Induction of Photosynthesis. Plant Physiol. 1993 Oct;103(2):649–60.

59. Michelet L, Zaffagnini M, Morisse S, Sparla F, Pérez-Pérez ME, Francia F, et al. Redox regulation of the Calvin-Benson cycle: something old, something new. Front Plant Sci. 2013 Nov 25;4:470.

60. Heldt WH, Werdan K, Milovancev M, Geller G. Alkalization of the chloroplast stroma caused by light-dependent proton flux into the thylakoid space. Biochim Biophys Acta. 1973 Aug 31;314(2):224–41.

61. Lichtenthaler HK, Buschmann C, Knapp M. How to correctly determine the different chlorophyll fluorescence parameters and the chlorophyll fluorescence decrease ratio R_{Fd} of leaves with the PAM fluorometer. Photosynthetica. 2005 Sep 1;43(3):379–93.

62. He S, Crans VL, Jonikas MC. The pyrenoid: the eukaryotic CO2-concentrating organelle. Plant Cell. 2023 Sep 1;35(9):3236–59.

63. Fei C, Wilson AT, Mangan NM, Wingreen NS, Jonikas MC. Modelling the pyrenoid-based CO-concentrating mechanism provides insights into its operating principles and a roadmap for its engineering into crops. Nat Plants. 2022 May;8(5):583–95.

64. Howitt CA, Vermaas WF. Quinol and cytochrome oxidases in the cyanobacterium Synechocystis sp. PCC 6803. Biochemistry. 1998 Dec 22;37(51):17944–51.

65. Berry S, Schneider D, Vermaas WFJ, Rögner M. Electron transport routes in whole cells of Synechocystis sp. strain PCC 6803: the role of the cytochrome bd-type oxidase. Biochemistry. 2002 Mar 12;41(10):3422–9.

66. Stirbet A, Govindjee. Chlorophyll a fluorescence induction: a personal perspective of the thermal phase, the J-I-P rise. Photosynth Res. 2012 Sep;113(1-3):15–61.

67. Short A, Fay TP, Crisanto T, Mangal R, Niyogi KK, Limmer DT, et al. Kinetics of the xanthophyll cycle and its role in photoprotective memory and response. Nat Commun. 2023 Oct 19;14(1):6621.

68. Gog L, Berenbaum MR, DeLucia EH. Mediation of Impacts of Elevated CO and Light Environment on Arabidopsis thaliana (L.) Chemical Defense against Insect Herbivory Via Photosynthesis. J Chem Ecol. 2019 Jan;45(1):61–73.

69. Joliot P, Johnson GN. Regulation of cyclic and linear electron flow in higher plants. Proc Natl Acad Sci U S A. 2011 Aug 9;108(32):13317–22.

70. Kern J, Chatterjee R, Young ID, Fuller FD, Lassalle L, Ibrahim M, et al. Structures of the intermediates of Kok's photosynthetic water oxidation clock. Nature. 2018 Nov;563(7731):421–5.

71. Sétif P. Electron-transfer kinetics in cyanobacterial cells: methyl viologen is a poor inhibitor of linear electron flow. Biochim Biophys Acta. 2015 Feb;1847(2):212–22.

72. Fuerst EP, Norman MA. Interactions of herbicides with photosynthetic electron transport. Weed Sci. 1991 Sep;39(3):458–64.

73. Yu L, Zhao J, Muhlenhoff U, Bryant DA, Golbeck JH. PsaE Is Required for in Vivo Cyclic Electron Flow around Photosystem I in the Cyanobacterium Synechococcus sp. PCC 7002. Plant Physiol. 1993 Sep;103(1):171–80.

74. Stokes DM, Walker DA. Photosynthesis by isolated chloroplasts. Inhibition by DL-glyceraldehyde of carbon dioxide assimilation. Biochem J. 1972 Aug;128(5):1147–57.

75. Pils D, Schmetterer G. Characterization of three bioenergetically active respiratory terminal oxidases in the cyanobacterium Synechocystis sp. strain PCC 6803. FEMS Microbiol Lett. 2001 Sep 25;203(2):217–22.

76. Redinbo MR, Yeates TO, Merchant S. Plastocyanin: structural and functional analysis. J Bioenerg Biomembr. 1994 Feb;26(1):49–66.

77. Hill R, Szabó M, ur Rehman A, Vass I, Ralph PJ, Larkum AWD. Inhibition of photosynthetic CO_2 fixation in the coral Pocillopora damicornis and its relationship to thermal bleaching. J Exp Biol. 2014 Jun 15;217(Pt 12):2150–62.

78. Tjus SE, Møller BL, Scheller HV. Photosystem I is an early target of photoinhibition in barley illuminated at chilling temperatures. Plant Physiol. 1998 Feb;116(2):755–64.

79. Sanakis Y, Petrouleas V, Diner BA. Cyanide binding at the non-heme Fe2+ of the iron-quinone complex of photosystem II: at high concentrations, cyanide converts the Fe2+ from high (S = 2) to low (S = 0) spin. Biochemistry. 1994 Aug 23;33(33):9922–8.

80. Miller NT, Vaughn MD, Burnap RL. Electron flow through NDH-1 complexes is the major driver of cyclic electron flow-dependent proton pumping in cyanobacteria. Biochim Biophys Acta Bioenerg. 2021 Mar 1;1862(3):148354.

81. Santos-Merino M, Torrado A, Davis GA, Röttig A, Bibby TS, Kramer DM, et al. Improved photosynthetic capacity and photosystem I oxidation via heterologous metabolism engineering in cyanobacteria. Proc Natl Acad Sci U S A [Internet]. 2021 Mar 16;118(11). Available from: http://dx.doi.org/10.1073/pnas.2021523118

82. Kusama S, Kojima S, Kimura K, Shimakawa G, Miyake C, Tanaka K, et al. Order-of-magnitude enhancement in photocurrent generation of Synechocystis sp. PCC 6803 by outer membrane deprivation. Nat Commun. 2022 Jun 2;13(1):3067.

83. Jahn M, Vialas V, Karlsen J, Maddalo G, Edfors F, Forsström B, et al. Growth of Cyanobacteria Is Constrained by the Abundance of Light and Carbon Assimilation Proteins. Cell Rep. 2018 Oct 9;25(2):478–86.e8.

84. Mustila H, Muth-Pawlak D, Aro EM, Allahverdiyeva Y. Global proteomic response of unicellular cyanobacterium Synechocystis sp. PCC 6803 to fluctuating light upon CO step-down. Physiol Plant. 2021 Sep;173(1):305–20.

85. Vermaas WF, Shen G, Styring S. Electrons generated by photosystem II are utilized by an

oxidase in the absence of photosystem I in the cyanobacterium Synechocystis sp. PCC 6803. FEBS Lett. 1994 Jan 3;337(1):103–8.

86. Fu A, Aluru M, Rodermel SR. Conserved active site sequences in Arabidopsis plastid terminal oxidase (PTOX): in vitro and in planta mutagenesis studies. J Biol Chem. 2009 Aug 21;284(34):22625–32.

87. Wishnick M, Lane MD. Inhibition of ribulose diphosphate carboxylase by cyanide. Inactive ternary complex of enzyme, ribulose diphosphate, and cyanide. J Biol Chem. 1969 Jan 10;244(1):55–9.

88. Berg SP, Krogmann DW. Mechanism of KCN inhibition of photosystem I. J Biol Chem. 1975 Dec 10;250(23):8957–62.

89. Tamary E, Kiss V, Nevo R, Adam Z, Bernát G, Rexroth S, et al. Structural and functional alterations of cyanobacterial phycobilisomes induced by high-light stress. Biochim Biophys Acta. 2012 Feb;1817(2):319–27.

90. Remelli W, Santabarbara S. Excitation and emission wavelength dependence of fluorescence spectra in whole cells of the cyanobacterium Synechocystis sp. PPC6803: Influence on the estimation of Photosystem II maximal quantum efficiency. Biochim Biophys Acta Bioenerg. 2018 Nov;1859(11):1207–22.

91. Tian L, van Stokkum IHM, Koehorst RBM, Jongerius A, Kirilovsky D, van Amerongen H. Site, rate, and mechanism of photoprotective quenching in cyanobacteria. J Am Chem Soc. 2011 Nov 16;133(45):18304–11.

92. Pfennig T, Kullmann E, Zavřel T, Nakielski A, Ebenhöh O, Červený J, et al. Shedding light on blue-green photosynthesis: A wavelength-dependent mathematical model of photosynthesis in Synechocystis sp. PCC 6803. PLoS Comput Biol. 2024 Sep;20(9):e1012445.

93. Wilson A, Ajlani G, Verbavatz JM, Vass I, Kerfeld CA, Kirilovsky D. A soluble carotenoid protein involved in phycobilisome-related energy dissipation in cyanobacteria. Plant Cell. 2006 Apr;18(4):992–1007.

94. Kanervo E, Mäenpää P, Aro EM. D1 Protein Degradation and psbA Transcript Levels in Synechocystis PCC 6803 during Photoinhibition in vivo. J Plant Physiol. 1993 Dec;142(6):669–75.

95. Vass I. Molecular mechanisms of photodamage in the Photosystem II complex. Biochim Biophys Acta. 2012 Jan;1817(1):209–17.

96. Bates H, Zavafer A, Szabó M, Ralph PJ. A guide to Open-JIP, a low-cost open-source chlorophyll fluorometer. Photosynth Res. 2019 Dec;142(3):361–8.

97. Schuurmans RM, Schuurmans JM, Bekker M, Kromkamp JC, Matthijs HCP, Hellingwerf KJ. The Redox Potential of the Plastoquinone Pool of the Cyanobacterium Synechocystis Species Strain PCC 6803 Is under Strict Homeostatic Control. Plant Physiol. 2014 Apr 2;165(1):463–75.

98. Espinoza-Corral R, Zavřel T, Sutter M, Leslie CH, Yang K, Beck WF, et al. The new phycobilisome linker protein ApcI regulates high light adaptation in*Synechocystis*sp. PCC 6803 [Internet]. bioRxiv. 2024. Available from: http://biorxiv.org/lookup/doi/10.1101/2024.09.09.612062

99. Kopecná J, Komenda J, Bucinská L, Sobotka R. Long-term acclimation of the cyanobacterium Synechocystis sp. PCC 6803 to high light is accompanied by an enhanced production of

chlorophyll that is preferentially channeled to trimeric photosystem I. Plant Physiol. 2012 Dec;160(4):2239–50.

100. Zavřel T, Faizi M, Loureiro C, Poschmann G, Stühler K, Sinetova M, et al. Quantitative insights into the cyanobacterial cell economy. Elife [Internet]. 2019 Feb 4;8. Available from: http://dx.doi.org/10.7554/eLife.42508

101. Zavřel T, Schoffman H, Lukeš M, Fedorko J, Keren N, Červený J. Monitoring fitness and productivity in cyanobacteria batch cultures. Algal Res. 2021 Jun;56(102328):102328.

102. Höper R, Komkova D, Zavřel T, Steuer R. A quantitative description of light-limited cyanobacterial growth using flux balance analysis. PLoS Comput Biol. 2024 Aug;20(8):e1012280.

103. Nikkanen L, Solymosi D, Jokel M, Allahverdiyeva Y. Regulatory electron transport pathways of photosynthesis in cyanobacteria and microalgae: Recent advances and biotechnological prospects. Physiol Plant. 2021 Oct;173(2):514–25.

104. Trinh MDL, Masuda S. Chloroplast pH Homeostasis for the Regulation of Photosynthesis. Front Plant Sci. 2022 May 25;13:919896.